

FERMILAB-PUB-97/205-T

LBNL-40466

UCB-PTH-97/34

RU-97-46

hep-ph/9706476

June 1997

## Signatures of multi-TeV scale particles in supersymmetric theories

Hsin-Chia Cheng<sup>1</sup>, Jonathan L. Feng<sup>2 \*</sup>, and Nir Polonsky<sup>3</sup>

<sup>1</sup> *Fermi National Accelerator Laboratory  
P. O. Box 500, Batavia, Illinois 60510*

<sup>2</sup> *Theoretical Physics Group, Lawrence Berkeley National Laboratory  
and Department of Physics, University of California, Berkeley, CA 94720*

<sup>3</sup> *Department of Physics and Astronomy  
Rutgers University, Piscataway, NJ 08855-0849*

### Abstract

Supersymmetric particles at the multi-TeV scale will escape direct detection at planned future colliders. However, such particles induce non-decoupling corrections in processes involving the accessible superparticles through violations of the supersymmetric equivalence between gauge boson and gaugino couplings. In a previous study, we parametrized these violations in terms of super-oblique parameters and found significant deviations in well-motivated models. Here, we systematically classify the possible experimental probes of such deviations, and present detailed investigations of representative observables available at a future linear collider. In some scenarios, the  $e^-e^-$  option and adjustable beam energy are exploited to achieve high precision. It is shown that precision measurements are possible for each of the three coupling relations, leading to significant bounds on the masses and properties of heavy superparticles and possible exotic sectors.

11.30.Pb 14.80.Ly

Typeset using REVTeX

---

\*Research Fellow, Miller Institute for Basic Research in Science.

## I. INTRODUCTION

If supersymmetry (SUSY) has relevance for the gauge hierarchy problem, fine-tuning considerations [1] suggest that supersymmetric particles typically have mass on order of or below the TeV scale. The discovery of some supersymmetric particles is therefore eagerly anticipated at present and future colliders. In particular, the Large Hadron Collider (LHC) [2] at CERN is likely to discover squarks and gluinos up to masses of  $1 - 2$  TeV [3–5], and proposed linear  $e^+e^-$  colliders [6–8], with  $\sqrt{s} = 0.5 - 1.5$  TeV, will be able to discover pair-produced superpartners with masses close to the kinematic limit [3,6,9,10].

It is possible, however, that some number of the superpartners of the standard model (SM) particles are heavy and beyond the discovery reach of planned future colliders. In fact, as will be described in more detail below, a wide variety of models predict superparticle spectra leading to such scenarios. If this possibility is actually realized in nature, we must then rely solely on indirect methods to probe the masses and properties of these heavy superparticles, at least until colliders at even higher energies become available. In most experimentally accessible processes, heavy supersymmetric states decouple, and their effects are not measurable for the large masses we are considering. However, the larger these masses are, the more they break SUSY, and so their effects may appear at detectable levels in processes involving light superpartners as violations of hard supersymmetric relations, *i.e.*, supersymmetric relations between dimensionless coupling constants. For example, consider the gauge couplings  $g_i$ , where the subscript  $i = 1, 2, 3$  refers to the U(1), SU(2), or SU(3) gauge group, and their SUSY counterparts, the gaugino-fermion-sfermion couplings, which we denote by  $h_i$ . In the limit of unbroken supersymmetry,

$$g_i = h_i . \tag{1}$$

However, the large SUSY breaking masses of heavy superpartners lead to deviations from these SUSY relations in the low energy effective theory where the heavy superpartners are decoupled. These deviations are non-decoupling and grow logarithmically with the heavy superpartner masses. In addition, Eq. (1) is model-independent and valid to all orders in the limit of unbroken SUSY. Deviations from the relations of Eq. (1) are therefore unambiguous signals of SUSY breaking mass splittings. Thus, the masses of kinematically inaccessible sparticles may be measured by precise determinations of such deviations from processes involving the accessible sparticles.

The corrections to Eq. (1) from split supermultiplets are very similar to the oblique corrections [11,12] from split SU(2) multiplets in the standard model. This analogy has been described in detail in a previous paper [13] and was noted in Ref. [14]. Ignoring Yukawa couplings, these corrections are dominantly from differences in the wavefunction renormalizations of gauge bosons and gauginos, which result from inequivalent loops after the decoupling of heavy superpartners. Such corrections are therefore most similar to those described by the  $U$  parameter of the oblique corrections [11], which is a measure of the difference between the wavefunction renormalizations of the  $W$  and  $Z$  gauge bosons arising from custodial isospin breaking masses in SU(2) multiplets. For this reason, in Ref. [13] we called the corresponding SUSY corrections “super-oblique corrections” and defined a set of “super-oblique parameters,”  $\tilde{U}_i$ , one for each gauge group, which measure deviations from Eq. (1). These parameters are given by [13]

$$\tilde{U}_i \equiv \frac{h_i(m)}{g_i(m)} - 1 \approx \frac{g_i^2(m)}{16\pi^2} (b_{g_i} - b_{h_i}) \ln \frac{M}{m} , \quad (2)$$

where  $M(m)$  is the heavy (light) superpartner scale, and  $b_{g_i}(b_{h_i})$  is the one-loop  $\beta$ -function coefficient for the gauge (gaugino) coupling in the effective theory between the heavy and light mass scales. Note that  $b_{g_i} > b_{h_i}$ , and so the super-oblique parameters are always positive (at the leading logarithm level) [13]. We also defined two-index parameters measuring the relative deviations of two gauge groups,

$$\tilde{U}_{ij} \equiv \frac{h_i(m)/h_j(m)}{g_i(m)/g_j(m)} - 1 \approx \tilde{U}_i - \tilde{U}_j . \quad (3)$$

The parameters  $\tilde{U}_{ij}$  are simple linear combinations of the  $\tilde{U}_i$ , but are physically relevant, as they are quantities that may be probed in branching ratio measurements, as we will see in an example below. These super-oblique parameters parametrize universal effects that enter all processes involving gaugino-fermion-sfermion interactions, and their simple form allows us to study such non-decoupling effects in a model-independent fashion. Other flavor-dependent non-decoupling corrections, for example, those induced by Yukawa couplings, and additional super-oblique corrections  $\tilde{T}_i$  were also described in Ref. [13]; we refer interested readers to that study for discussion of these and other issues.

Depending on which superpartners are heavy, the models that contain heavy superparticles may be roughly divided into two categories [13]: “heavy QCD models” and “2–1 models.” In heavy QCD models, all strongly-interacting superpartners, *i.e.*, the gluino and all squarks, are in the heavy sector. Their large SUSY breaking masses may arise from either the proportionality of soft masses to standard model gauge coupling constants or the renormalization group evolution effects of a large gluino mass. Examples of such models include the no-scale limit of minimal supergravity [15], models of gauge-mediated SUSY breaking [16], and models with non-universal gaugino masses and a heavy gluino [17]. The super-oblique corrections in these models have been calculated in Ref. [13], and the results are

$$\tilde{U}_2 \approx 0.80\% \times \ln R , \quad (4)$$

$$\tilde{U}_1 \approx 0.29\% \times \ln R , \quad (5)$$

$$\tilde{U}_{21} \approx 0.50\% \times \ln R , \quad (6)$$

where  $R = M/m$  is typically  $\mathcal{O}(10)$  in heavy QCD models.

In 2–1 models, the scalars of the first two generations are heavy and the third generation scalars are at the weak scale [18]. These models are motivated by attempts to solve the SUSY flavor problem with heavy first two generation scalars while avoiding extreme fine-tuning problems by keeping the third generation scalars, which couple strongly to the Higgs sector, at the weak scale. Assuming all gauginos to be in the light sector, the super-oblique corrections in 2–1 models were found in Ref. [13] to be

$$\tilde{U}_3 \approx 2.5\% \times \ln R , \quad (7)$$

$$\tilde{U}_2 \approx 0.71\% \times \ln R , \quad (8)$$

$$\tilde{U}_1 \approx 0.35\% \times \ln R , \quad (9)$$

$$\tilde{U}_{32} \approx 1.8\% \times \ln R , \quad (10)$$

$$\tilde{U}_{31} \approx 2.2\% \times \ln R , \quad (11)$$

$$\tilde{U}_{21} \approx 0.35\% \times \ln R . \quad (12)$$

In 2–1 models, values of  $R$  in the range  $\sim 40 - 200$  may be taken as typical.

Although the values of expected super-oblique parameters vary from model to model, they are always proportional to the square of their corresponding standard model gauge couplings, as is clear from Eq. (2). Thus, we typically expect the parameters  $\tilde{U}_3$ ,  $\tilde{U}_{31}$ , and  $\tilde{U}_{32}$  to be the largest, and, for example, a 1% measurement of  $\tilde{U}_2$  is more powerful than a 1% measurement of  $\tilde{U}_1$  for the purposes of bounding new physics scales. Finally, note that extra vector-like fields with both SUSY preserving and SUSY breaking masses, such as the messengers in gauge mediation models, may also contribute to the super-oblique parameters. Such contributions were also calculated in Ref. [13], and were found to be typically small, with significant contributions only for very highly split supermultiplets.

The possibility of measuring the supersymmetric couplings  $h_i$  and testing the relations  $g_i = h_i$  has been discussed previously. In the original proposal [19], the possibility of testing the SU(2) relation through chargino production at the Next Linear Collider (NLC) was explored. Here the focus was on establishing the identity of new particles as superpartners through the verification of SUSY relations. A test of the U(1) relation through  $e^+e^- \rightarrow \tilde{e}_R^+ \tilde{e}_R^-$  was considered in Ref. [20]. In this study, both the possibilities of verifying SUSY relations and of being sensitive to deviations arising from heavy sparticle thresholds were considered. Corrections to hard supersymmetry relations were previously studied in Ref. [21], where deviations in squark widths were calculated. However, the possibility of experimentally verifying such deviations was not addressed.

In this paper, we will systematically classify the many experimental observables that depend on the couplings  $h_i$  and are therefore formally candidates for measuring super-oblique parameters. We then consider three representative examples of observables that may be sufficiently sensitive to such parameters to yield interesting results. Even after including many experimental errors and the theoretical uncertainties arising from the plethora of unknown SUSY parameters, we find some promising prospects for very high precision measurements. The results have implications for collider design, as certain options, particularly the  $e^+e^-$  mode and adjustable beam energies, will be seen to be particularly useful. It is important to note that a complete study will require detailed experimental simulations appropriate to the particular scenario realized in nature, and the case studies we consider typically require measurements beyond the first stage of experimental study. However, given that the measurements discussed here may be the only experimental window on physics beyond the TeV scale for the foreseeable future, such issues are well worth investigation.

We begin in Sec. II by identifying the many experimental observables that may possibly be used to detect variations in the hard SUSY relations. Of course, not all of these observables may be measured precisely enough to provide significant bounds on heavy superpartner masses. In Sec. III we discuss the many uncertainties, both experimental and theoretical, that appear in any measurement, and we describe our treatment of these errors. In Secs. IV–VI, detailed discussions of the precisions achievable are given for three representative examples, one for each coupling constant relation. In Sec. IV, we will find that chargino production at the NLC gives bounds on the heavy mass scale comparable to

those achieved from  $e^+e^- \rightarrow \tilde{e}_R^+ \tilde{e}_R^-$  in Ref. [20]. In Sec. V, we improve upon both of these results by considering selectron production in the  $e^-e^-$  mode, where a number of beautiful properties may be exploited to reach very high precision. Finally, in Sec. VI, we find that significant constraints on the SU(3) super-oblique parameter may also be possible from squark branching ratios in particular regions of parameter space. These examples are by no means exhaustive. However, they make use of three different sets of sparticles, and are presented to emphasize the variety of precise probes that may be used to provide interesting bounds. The numerous implications of such measurements are collected in Sec. VII.

## II. OBSERVABLE PROBES OF SUPER-OBLIQUE CORRECTIONS

As seen in the previous section, heavy superpartners may induce significant corrections to all three coupling constant relations  $g_i = h_i$ . We now discuss what observables at colliders have dependences on the couplings  $h_i$  and are therefore candidates for testing these relations and determining the super-oblique parameters. In this section, we will concentrate on measuring the couplings  $h_i$  at the light superparticle mass scale  $m$ . Such measurements allow one to measure the heavy sparticle mass scale  $M$ . Of course, measurements of  $h_i$  at higher momentum transfers  $p^2 > m^2$  may also be extremely useful, and would allow one to verify the convergence of  $\tilde{U}_i \rightarrow 0$  as  $p^2 \rightarrow M^2$ .<sup>1</sup> Here, however, we will focus on the classification and measurement of observables at  $p^2 = m^2$ , leaving the latter for future studies. We begin with observables at  $e^+e^-$  (and  $e^-e^-$ ) colliders, where the ability to make precise model-independent measurements of a wide variety of SUSY parameters is most promising. The  $e^+e^-$  observables all have analogues at hadron colliders, and we then turn to hadron colliders and discuss briefly which of these appear most promising in that experimental environment. Analogous observables may also be found at a  $\mu^+\mu^-$  collider, with appropriate and obvious replacements of selectrons by smuons in the case of electroweak observables.

### A. Observables at $e^+e^-$ Colliders

Each kinematically accessible superpartner brings with it a set of observables. We consider each superpartner in turn, grouping together those that are similar for this analysis.

#### 1. Charginos and Neutralinos

If charginos are kinematically accessible, their production cross sections are possible probes. This applies formally to all reactions, ranging from chargino pair production to more unusual processes where charginos are produced in association with other particles, such as in  $\tilde{\chi}^\pm e^\mp \tilde{\nu}$  production. In the most obvious and useful example, charginos are pair-produced in  $e^+e^-$  collisions through  $s$ -channel  $\gamma$  and  $Z$  diagrams and  $t$ -channel sneutrino exchange. The latter diagram depends on the coupling  $h_2$ , and so chargino pair production

---

<sup>1</sup>We thank X. Tata for this proposal.

cross sections may be used to measure the parameter  $\tilde{U}_2$ . In fact, this will serve as our first example in Sec. IV. If charginos have two or more open decay modes, their branching fractions may also be used.<sup>2</sup> For example, if decays  $\tilde{\chi}^\pm \rightarrow \tilde{f} f'$  and  $\tilde{\chi}^\pm \rightarrow W^\pm \tilde{\chi}^0$  are both open, the ratio of these branching fractions is dependent on  $h_2^2/g_2^2$  (if the chargino is pure Wino) and may serve as a probe as well.

For neutralinos, the situation is similar. Neutralino pair production cross sections depend on  $h_1$  and  $h_2$  through diagrams with  $t$ -channel  $\tilde{e}$  exchange. Their branching fractions are also accessible probes when two or more decay modes are competitive.

An interesting effect of the super-oblique corrections for charginos and neutralinos is the modification of their mass matrices. For example, the conventional chargino mass terms are  $(\psi^-)^T \mathbf{M}_{\tilde{\chi}^\pm} \psi^+ + \text{h.c.}$ , where  $(\psi^\pm)^T = (-i\tilde{W}^\pm, \tilde{H}^\pm)$  and

$$\mathbf{M}_{\tilde{\chi}^\pm} = \begin{pmatrix} M_2 & \sqrt{2} m_W \sin \beta \\ \sqrt{2} m_W \cos \beta & \mu \end{pmatrix}. \quad (13)$$

Here  $M_2$  is the SU(2) gaugino mass,  $\tan \beta$  is the ratio of Higgs vacuum expectation values, and  $\mu$  is the Higgsino mass parameter. The off-diagonal entries of the mass matrix result from the interactions  $H\tilde{W}\tilde{H}$ . In the presence of super-oblique corrections, these entries must be modified by  $m_W \rightarrow (h_2/g_2)m_W$ . Similar comments apply to the neutralino mixing matrix. Thus, precise measurements of the chargino and neutralino masses and mixings may also yield bounds on the super-oblique parameters. Such precision measurements were in fact studied for charginos in Ref. [19]. In the mixed region, where there is large gaugino-Higgsino mixing, interesting bounds may be obtained, although measurements of the super-oblique parameters at the percent level appear difficult. However, in the regions of parameter space in which charginos and neutralinos are nearly pure gauginos or Higgsinos, the dependence on the off-diagonal terms is small, and the effects of super-oblique parameters through the mass matrices are negligible.

Before considering other sparticles, a few comments are in order. First, it is clear that no tests are applicable in all regions of parameter space. For the observables above to be sensitive to the super-oblique parameters, for example, it is necessary not only that charginos and neutralinos be produced, but also that they have either large gaugino components or substantial gaugino-Higgsino mixing. Second, all observables depend on many additional SUSY parameters, including, for example, the masses and compositions of the charginos and neutralinos, and the masses of the sfermions entering the process. Thus, a determination of  $h_i$  requires a simultaneous determination of many other parameters. This is one of the essential difficulties in these analyses, and will be addressed in detail in the case studies of the following sections.

---

<sup>2</sup>Of course, individual decay widths may also depend on the couplings  $h_i$ . In special circumstances, such as when the decays are extremely suppressed and the decay lengths are macroscopic, the widths themselves may be measurable. In general, however, individual decay widths are very difficult to measure, and we will therefore concentrate on their ratios in the following.

## 2. First Generation Sleptons

For measurements of super-oblique parameters, selectrons  $\tilde{e}_{L,R}$  and electron sneutrinos  $\tilde{\nu}_e$  afford special opportunities. For example, selectron pair-production cross sections receive contributions from  $t$ -channel neutralino exchange, and so the  $\tilde{e}_R\tilde{e}_R$  and  $\tilde{e}_R\tilde{e}_L$  cross sections depend on  $h_1$ , while the  $\tilde{e}_L\tilde{e}_L$  cross section depends on both  $h_1$  and  $h_2$ . This dependence was exploited in Ref. [20] to measure  $h_1$  at  $e^+e^-$  colliders. Note, however, that selectrons, unlike gauginos, may also be produced in pairs in  $e^-e^-$  collisions. Such reactions may lead to particularly precise measurements and will be discussed in detail in Sec. V. Selectron branching fractions may also be useful when two decay modes are open. For example, the ratio  $B(\tilde{e}_L \rightarrow e\tilde{W})/B(\tilde{e}_L \rightarrow e\tilde{B})$  depends on  $h_2^2/h_1^2$ , and may therefore be used to probe  $\tilde{U}_{21}$ .

Electron sneutrinos may also be produced in  $e^+e^-$  collisions. Their production cross sections receive contributions from  $t$ -channel chargino exchange, and so are sensitive to  $h_2$ . Their branching ratios may also be used.

## 3. Squarks, Gluinos, Higgses, and Other Sleptons

If gluinos and the other scalars (squarks, Higgs bosons, and second or third generation sleptons) are accessible, they may also provide useful information. Cross sections for production in association with gauginos, for example,  $\sigma(e^+e^- \rightarrow \tilde{q}\tilde{q}\tilde{g})$ , depend on  $h_i$  couplings. In addition, as with the other particles, their branching ratios are also possible probes. We will consider the case of squark branching ratios in Sec. VI.

## B. Observables at Hadron Colliders

All of the observables mentioned above have analogues at hadron colliders. A promising aspect of hadron colliders is that strongly interacting sparticles may be produced in great numbers, allowing probes of the QCD relations, where the greatest deviations are expected. The production cross sections of gluinos and squarks are dependent on the couplings  $h_i$ . Unfortunately, cross section measurements at hadron colliders are open to systematic uncertainties that, at the level of precision we require for this study, make such measurements rather difficult. On the other hand, branching ratios may be well measured. For example, if squarks may decay to both gluinos and electroweak gauginos, the relative rates may be a sensitive probe of the super-oblique corrections. Similar comments apply to sleptons and electroweak gauginos when more than one decay path is open. The extent to which these branching ratios may be measured depends strongly on the efficiency for extracting these signals from background, and is dependent on many SUSY parameters. In this study, we will concentrate on  $e^+e^-$  probes, although, given the exciting prospects for discovering SUSY at the LHC, probes there certainly merit attention, especially if portions of the sparticle spectrum are not observed or branching ratios deviate from expectations.

### C. Probes of other non-decoupling corrections

So far we have concentrated on observables involving gaugino interactions as probes of the super-oblique corrections. In fact, however, heavy superpartner sectors may also induce non-decoupling effects in interactions that do not involve gauginos. In particular, as discussed in Ref. [13],  $D$ -term quartic scalar couplings also receive corrections. Such corrections appear in a wide variety of observables.

Nevertheless, they are generically highly challenging to probe experimentally. To begin with, the couplings of four physical scalars are extremely difficult to measure. However,  $D$ -term couplings also result in cubic scalar couplings when one field is a Higgs. These appear in more accessible observables, including, for example, the widths of heavy Higgs boson decays to sfermions  $H, A \rightarrow \tilde{f}\tilde{f}^*$  and  $H^\pm \rightarrow \tilde{f}\tilde{f}'$ . (Note that the  $D$ -term trilinear terms discussed here involve same-chirality sfermions and are not suppressed by Yukawa couplings; they may thereby be distinguished from Yukawa-suppressed trilinear terms that originate from  $F$ -terms or from soft SUSY breaking trilinear interactions.) Unfortunately, in the models we are considering, heavy Higgs bosons may be very heavy, since their mass is governed by  $\mu$ , which, given the constraint of the  $Z$  boson mass, is typically at the third generation squark mass scale. In addition, heavy Higgs bosons are difficult to study at hadron colliders, and their interactions depend on a number of other parameters, such as  $\tan\beta$  and the  $CP$ -even Higgs mixing angle  $\alpha$ . Finally,  $D$ -terms contribute to  $SU(2)$  doublet mass splittings, such as the splitting between  $m_{\tilde{e}_L}$  and  $m_{\tilde{\nu}_e}$ . However, these contributions are only small fractional deviations in already small mass splittings. In summary, the  $D$ -term non-decoupling effects may be relevant in certain scenarios, for example, if a heavy Higgs is accessible at an  $e^+e^-$  collider. However, they do not generally appear promising as probes of heavy sector physics. In the following sections, we will therefore concentrate on measurements of the super-oblique corrections through the observables described above, that is, in processes involving gauginos.

### III. UNCERTAINTIES IN OBSERVABLES

Having now identified a large list of possible observables that depend on the SUSY couplings  $h_i$ , we must determine if some of these may be measured precisely enough to be significant probes of the heavy sparticle sector. In the sections that follow, we will consider such quantitative issues in three examples that are representative in the sense that there is one example for each coupling constant relation, and one example for each of the three groups of particles given in Sec. II A. Here, however, we give a general description of the various errors that enter such analyses and our treatment of these errors.

The uncertainties may be grouped into categories. First, there are uncertainties arising from the many unknown SUSY parameters that enter any given analysis. These we will call theoretical systematic uncertainties. If, for example, a measurement of super-oblique parameters is to be obtained from a cross section that depends on  $h_i$ , the other parameters entering the cross section must be carefully controlled. These parameters include the masses of the particles involved, as well as the field content of these particles, for example, the gaugino content of relevant charginos and neutralinos. We will carefully study these errors, and



will find that, by appealing to other measurements and exploiting various collider features, such uncertainties may be reduced to promisingly low levels.

There are also uncertainties from finite experimental statistics and backgrounds. These will also be included, and we will present results for specific integrated luminosities. We assume that the backgrounds are well-understood and so may be subtracted up to statistical uncertainties. This is a reasonable assumption for standard model backgrounds. Of course, for certain regions of parameter space, SUSY backgrounds may enter. These depend on *a priori* unknown SUSY parameters, and the uncertainties associated with these are then part of the first category discussed above.

In our analyses, we have not included radiative corrections in our calculations of cross sections and branching ratios. The large logarithm radiative corrections are absorbed in the super-oblique parameters we are hoping to probe. There remain, however, radiative corrections from standard model particles, as well as the accessible superpartners. At the level of precision we will be considering, these effects may be important. However, these corrections are in principle well-known once the calculations appropriate to the scenario actually realized in nature are completed and a consistent one-loop regularization scheme is established for all relevant observables. Radiative corrections dependent on the light superparticles will be subject to theoretical systematic uncertainties, but these are small relative to the theoretical systematic uncertainties entering at tree level, which were described above and will be included in our analyses.

The final group of uncertainties are experimental systematic errors. These include, for example, uncertainties in luminosity, detector acceptances, initial state radiation effects, and, in some of the measurements considered below, beam polarization and *b*-tagging efficiency. A complete analysis would require detailed experimental simulations incorporating all of these experimental systematic uncertainties. Such an analysis is beyond the scope of this work, especially since the sizes of some of these uncertainties at the NLC are unknown and are currently under investigation. We will see, however, that in some cases the experimental systematic uncertainties are likely to be negligible relative to the errors described above; where this is not the case, we will note which experimental systematic errors appear to be most important. By estimating the sizes of the errors from the sources described in the paragraphs above, we will find interesting implications for what collider specifications are required and what features are particularly promising for the study of non-decoupling SUSY breaking effects.

#### IV. PROBE OF SU(2) COUPLINGS FROM CHARGINOS

In this section, we consider a probe of the SU(2) relation  $g_2 = h_2$ . Recall from Sec. I that the size of deviations from this equivalence may be parametrized by the super-oblique parameter  $\tilde{U}_2$ , which, in the two scenarios we considered, is

$$\tilde{U}_2 \equiv h_2/g_2 - 1 \approx 0.7 - 0.8\% \times \ln \frac{M}{m} . \quad (14)$$

For a light sector scale  $m \approx \mathcal{O}(100 \text{ GeV})$ , we see that measurements of  $\tilde{U}_2$  to accuracies of 3–4% are required to be sensitive to deviations from a heavy scale  $M \approx \mathcal{O}(10 \text{ TeV})$ , while

determination of the heavy scale to within a factor of 3 requires measurements at the 0.8–0.9% level. Of course, larger deviations from greater  $M$  or additional exotic supermultiplets are possible, but we will take these figures as useful reference points.

As a test of the SU(2) coupling relation, we turn to the first group of sparticles given in Sec. II, charginos and neutralinos, and consider chargino pair production at the NLC. This process is promising, as charginos are typically among the lighter sparticles, and they are produced with large cross section when kinematically accessible. In addition, in our scenarios, the constraint of the  $Z$  mass implies that the Higgsino mass parameter  $|\mu|$  is usually of order the third generation squark masses. This often implies that the lighter chargino and neutralinos are gaugino-like, and is exactly the region of parameter space where we have some hope of measuring  $h_2$  accurately with charginos, as explained in Sec. II.

The measurement of  $h_2$  from chargino production was previously considered in Ref. [19], and we therefore begin with a review of those results. Details, particularly those concerning the error analysis, will be omitted, and we refer interested readers to the original study for a complete treatment. In Ref. [19], the following parameters were taken as a case study in the gaugino region:

$$(\mu, M_2, \tan \beta, M_1/M_2, m_{\tilde{\nu}_e}) = (-500 \text{ GeV}, 170 \text{ GeV}, 4, 0.5, 400 \text{ GeV}) . \quad (15)$$

With these parameters, the light chargino and neutralino masses are  $m_{\tilde{\chi}_1^\pm} = 172 \text{ GeV}$  and  $m_{\tilde{\chi}_1^0} = 86 \text{ GeV}$ , and the cross sections for chargino pair production with  $\sqrt{s} = 500 \text{ GeV}$ , unpolarized  $e^+$  beams, and right- and left-polarized  $e^-$  beams are  $\sigma_R = 0.15 \text{ fb}$  and  $\sigma_L = 612 \text{ fb}$ . As is characteristic of the gaugino region,  $\sigma_R$  is highly suppressed, but  $\sigma_L$  is large. With design luminosity  $\mathcal{L} = 50 \text{ fb}^{-1}/\text{yr}$ , tens of thousands of charginos will be produced each year, giving us hope that  $\mathcal{O}(1)\%$  measurements may be feasible. Finally, the decay  $\tilde{\chi}_1^\pm \rightarrow W^\pm \tilde{\chi}_1^0$  is open and dominant — the chargino branching ratios are therefore equivalent to those of the  $W$ .<sup>3</sup>

Charginos may be produced through  $t$ -channel sneutrino exchange and  $s$ -channel  $\gamma$  and  $Z$  diagrams. The first amplitude depends on  $h_2^2$ , and is the source of our sensitivity to super-oblique corrections. The left-polarized differential cross section is therefore dependent on 5 parameters beyond the standard model:

$$\frac{d\sigma}{d\cos\theta} (e^- e^+ \rightarrow \tilde{\chi}_1^+ \tilde{\chi}_1^-) = \frac{d\sigma}{d\cos\theta} (m_{\tilde{\chi}^\pm}, \phi_+, \phi_-, m_{\tilde{\nu}_e}, h_2) , \quad (16)$$

where the angles  $\phi_\pm$  specify the composition of  $\tilde{\chi}_1^\pm$  in terms of the weak eigenstates  $(-i\tilde{W}^\pm, \tilde{H}^\pm)$ . To measure  $h_2$ , we must also constrain the other parameters. The mass  $m_{\tilde{\chi}_1^\pm}$  may be measured to 2 GeV by determining energy distribution endpoints of the decay products [6]. The Wino-ness of the chargino may be established by checking that  $\sigma_R \approx 0$ .

---

<sup>3</sup>For extremely large values of  $|\mu|$ , the chargino and neutralino are nearly pure gauginos, and the on-shell  $W$  decay mode may be so suppressed that decays through off-shell sleptons and squarks significantly shift the chargino branching ratios. We will not consider this case, but note that such a scenario typically requires values of  $|\mu|$  far above the TeV scale and would itself be a striking signature for heavy mass scales.

Alternatively, one can verify that  $\tilde{\chi}_1^\pm \tilde{\chi}_2^\mp$  production is kinematically inaccessible, which puts lower limits on  $|\mu|$  and the gaugino-ness of the chargino. (Of course, if higher beam energy is available, one could discover the heavy chargino or neutralinos and measure  $|\mu|$  and the angles  $\phi^\pm$ .) The resulting errors in  $m_{\tilde{\chi}_1^\pm}$  and  $\phi_\pm$  at a  $\sqrt{s} = 500$  GeV machine were studied in Ref. [19] and were found to be negligible relative to the uncertainties we now describe.

The remaining two unknowns,  $m_{\tilde{\nu}_e}$  and  $h_2$ , may then be determined by the  $e_L^-$  total cross section  $\sigma_L$  and a truncated forward-backward asymmetry

$$A_L^\chi = \frac{\sigma_L(0 < \cos \theta < 0.707) - \sigma_L(-1 < \cos \theta < 0)}{\sigma_L(-1 < \cos \theta < 0.707)}. \quad (17)$$

This peculiar definition of  $A_L^\chi$  is dictated by cuts designed to remove the forward-peaked  $W$  pair production. These two quantities are plotted in Figs. 1 and 2 for  $\sqrt{s} = 500$  GeV. Unfortunately, these quantities cannot be measured directly. To determine them, we look at mixed mode events, where one chargino decays hadronically and the other leptonically.  $A_L^\chi$  is measured through its correlation with the observed forward-backward asymmetry of the hadronic decay products  $A^{\text{had}}$ , and the total cross section is determined by its correlation with the measured mixed mode cross section after cuts. Both of these correlations are imperfect. The correlation between  $A^{\text{had}}$  and  $A_L^\chi$  has a slight dependence on additional SUSY parameters entering the decay, such as  $M_1$ . The total cross section determination is weakened by its dependence on the cut efficiencies, which also depend on these additional SUSY parameters.<sup>4</sup> These effects lead to theoretical systematic errors, which are investigated by Monte-Carlo simulations, where the lack of correlation is determined by varying all the relevant SUSY parameters throughout their ranges, subject only to the constraint that they reproduce various observables, such as the chargino mass, within the experimental errors.

In addition to these theoretical systematic errors, uncertainties from backgrounds, dominated by  $WW$  production, and finite statistics must be included. The resulting  $1\sigma$  uncertainties are [19]

$$\begin{aligned} \Delta A_L^\chi &= 0.067 (0.048) [0.037] \\ \frac{\Delta \sigma_L}{\sigma_L} &= 7.2 (5.6) [4.7]\%, \end{aligned} \quad (18)$$

where the first two uncertainties are for integrated luminosities of 30 (100)  $\text{fb}^{-1}$ , and the final bracketed uncertainties are from systematic errors alone, *i.e.*, the uncertainties in the limit of infinite statistics. Given these values, the expected  $\sim 1\%$  uncertainty in luminosity [6] is negligible. If similar uncertainties in beam polarization may be obtained, they too have little impact. In any case, note that beam polarization is used here only to increase the effective luminosity for this study, as the signal and leading  $WW$  background both exist only for left-polarized beams. Thus, if polarization uncertainties are dominant, the systematic error

---

<sup>4</sup>Note that the determination of the total cross section from the mixed cross section also requires that the chargino branching fractions be known. If decays through on-shell  $W$  bosons are closed, the branching ratios must also be determined by considering the purely hadronic or purely leptonic modes, introducing additional uncertainties that may significantly weaken the results.

from this source may be eliminated by using an unpolarized beam, with a resultant decrease in effective luminosity by a factor of 2.

The measurements of Eq. (18) determine allowed regions in the  $(m_{\tilde{\nu}_e}, h_2)$  plane, which we define crudely to be regions that are within the  $1\sigma$  contours of all observables. The relevant region for integrated luminosity  $100 \text{ fb}^{-1}$  is given in Fig. 3. Even without a measurement of  $m_{\tilde{\nu}_e}$ , we see that the ratio  $h_2/g_2$  is constrained to be consistent with unity, a quantitative confirmation of SUSY and the interpretation that the fermion being studied is in fact the chargino.

The measurements at  $\sqrt{s} = 500 \text{ GeV}$  also bound the sneutrino's mass through its virtual effects. With this strong motivation, one would then increase the beam energy to find  $\tilde{\nu}_e$  pair production. Studies have found that  $\sim 1\%$  measurements of charged slepton masses are possible at the NLC [22], and similar levels have been achieved in sneutrino studies through measurements of electron energies in the decay  $\tilde{\nu}_e \rightarrow e^\mp \tilde{\chi}_1^\pm$  [10]. With this as an additional constraint, we may return to Fig. 3 and look for small deviations from  $g_2 = h_2$ . We see that, for example, if  $m_{\tilde{\nu}_e}$  is measured to 4 GeV, deviations of  $\tilde{U}_2$  from its central value are constrained to the range

$$-3\% < \Delta\tilde{U}_2 < 3\% \quad (m_{\tilde{\nu}_e} = 400 \text{ GeV}, \sqrt{s} = 500 \text{ GeV}) . \quad (19)$$

At this parameter point, the determination is sufficiently accurate that to good approximation, the uncertainties are linear, *i.e.*, if the underlying value of  $\tilde{U}_2$  is 4%, the allowed range is  $1\% < \tilde{U}_2 < 7\%$ . Thus, if the mass of squarks is  $\gtrsim \mathcal{O}(10 \text{ TeV})$ , deviations from exact SUSY may be seen and  $\tilde{U}_2$  may be bounded to be positive. Such a measurement would provide unambiguous evidence for very massive superparticle states. Note, however, that the mass scale of such states is determined only to a couple of orders of magnitude.

In fact, the precision of the above study may be improved by exploiting an important feature of the NLC, its adjustable beam energy. To illustrate this most vividly, let us consider another point in parameter space with a different sneutrino mass. In Ref. [19], a large  $m_{\tilde{\nu}_e}$  was chosen to illustrate the sensitivity of precision measurements to effects of virtual sparticles. For  $\sqrt{s} = 500 \text{ GeV}$  and  $m_{\tilde{\nu}_e} = 400 \text{ GeV}$ ,  $\sigma_L$  and  $A_L^X$  are quite sensitive to changes in  $h_2$  and  $m_{\tilde{\nu}_e}$ . However, for other underlying parameters, this may not be the case. For example, we see in Figs. 1 and 2 that, for  $\sqrt{s} = 500 \text{ GeV}$  and  $m_{\tilde{\nu}_e} = 240 \text{ GeV}$ ,  $\sigma_L$  is near a minimum and  $A_L^X$  is near a saddle point at  $h_2 = g_2$ . Thus for such a sneutrino mass, there are relatively few events, and more importantly, the dependence of our observables on  $h_2$  is weak. By carrying out the analysis outlined above for this new parameter point, we find

$$\begin{aligned} \Delta A_L^X &= 0.079 (0.053) \\ \frac{\Delta\sigma_L}{\sigma_L} &= 9.4 (6.2)\% , \end{aligned} \quad (20)$$

where these  $1\sigma$  uncertainties are for integrated luminosities of 30 (100)  $\text{fb}^{-1}$ . (We have assumed here that the theoretical systematic errors in this case are as in the previous  $m_{\tilde{\nu}_e} = 400 \text{ GeV}$  analysis. This assumption is valid, as these uncertainties are not dominant, and are in any case most sensitive to quantities, such as the chargino velocity, that are identical in these two case studies.) In Fig. 4, we plot the region allowed by these measurements. The

determination of  $\tilde{U}_2$  is greatly deteriorated. If  $m_{\tilde{\nu}_e}$  is again measured to  $\sim 1\%$ , the range of  $\tilde{U}_2$  in the allowed region is (taking a central value of  $\tilde{U}_2 = 0$ )

$$-5\% < \tilde{U}_2 < 8\% \quad (m_{\tilde{\nu}_e} = 240 \text{ GeV}, \sqrt{s} = 500 \text{ GeV}) . \quad (21)$$

The underlying SUSY parameters above appear to lead to poor bounds on super-oblique corrections. However, an important aspect of  $e^+e^-$  colliders is the ability to adjust the initial state parton energy. This flexibility may be used to eliminate backgrounds, and also to improve the sensitivity to underlying parameters. Here, we exploit the latter virtue. The extrema in  $\sigma_L$  and  $A_L^\chi$  may be shifted by choosing different beam energies. In Figs. 5 and 6, we plot  $\sigma_L$  and  $A_L^\chi$  in the  $(m_{\tilde{\nu}_e}, h_2)$  plane again, but now for  $\sqrt{s} = 400$  GeV. We see that the extrema in the  $\sigma_L$  and  $A_L^\chi$  observables are shifted to lower  $m_{\tilde{\nu}_e}$ , and the strong dependence of  $\sigma_L$  and  $A_L^\chi$  on  $h_2$  for  $m_{\tilde{\nu}_e} = 240$  GeV is restored. Applying the same analysis once again, we find, including all theoretical systematic and experimental statistical errors,

$$\begin{aligned} \Delta A_L^\chi &= 0.11 \text{ (0.068)} \\ \frac{\Delta \sigma_L}{\sigma_L} &= 11 \text{ (7.3)\%} , \end{aligned} \quad (22)$$

for integrated luminosities of 30 (100)  $\text{fb}^{-1}$ .<sup>5</sup> We see that these uncertainties are larger than at  $\sqrt{s} = 500$  GeV. However, the increased sensitivity of  $\sigma_L$  and  $A_L^\chi$  to  $h_2/g_2$  more than makes up for the loss in statistics, as can be seen in Fig. 7, where we plot the allowed region for underlying parameters as in Fig. 4, but for  $\sqrt{s} = 400$  GeV. Assuming again a  $\sim 1\%$  measurement of  $m_{\tilde{\nu}_e}$ , the range of allowed deviations of  $\tilde{U}_2$  from its central value in the allowed region is

$$-2\% < \Delta \tilde{U}_2 < 2\% \quad (m_{\tilde{\nu}_e} = 240 \text{ GeV}, \sqrt{s} = 400 \text{ GeV}) , \quad (23)$$

where again we have checked that the uncertainties are linear. Such a measurement gives one an extremely precise measurement of  $h_2$ , and even begins to provide interesting constraints on the heavy squark scale for the purposes of model-building. Note that this bound from charginos is comparable to the previous bound derived from selectron production in the  $e^+e^-$  mode of linear colliders [20]. The bound from selectron production was  $\sim 1\%$  on the parameter  $\tilde{U}_1$ , which we expect in typical models to be roughly half as sensitive to the effects of heavy superpartners.

Although a complete scan of parameter space is beyond the scope of this study, we see that if gaugino-like charginos are produced at the NLC, interesting bounds on the super-oblique parameter  $\tilde{U}_2$  may be obtained. Such bounds rely on a variety of precise measurements constraining the gaugino content of the chargino and the  $\tilde{\nu}_e$  mass. In addition, we have

---

<sup>5</sup>In arriving at these results, we have not designed optimized cuts for  $\sqrt{s} = 400$  GeV, but have simply assumed that the efficiency of the cuts for the  $WW$  background is unchanged at  $\sqrt{s} = 400$  GeV. The results are rather insensitive to this assumption; for example, making the highly pessimistic assumption that the background is in fact doubled leads to  $\Delta A_L^\chi = 0.083$  and  $\frac{\Delta \sigma_L}{\sigma_L} = 8.9\%$  for 100  $\text{fb}^{-1}$ .

seen that the sensitivity of observables to the super-oblique parameters may be markedly improved by adjusting the beam energy. Given a better understanding of the uncertainties obtainable in the sneutrino mass and various experimental systematic uncertainties, the beam energy may be optimized to increase the sensitivity to super-oblique corrections and multi-TeV superpartners.

## V. PROBE OF U(1) COUPLINGS FROM SELECTRONS

In this section, we consider measurements of the U(1) gaugino coupling  $h_1$  from selectron production. From Sec. I, we see that the deviation between the U(1) gauge boson and gaugino couplings for the heavy QCD and 2-1 models is

$$\tilde{U}_1 \equiv h_1/g_1 - 1 \approx 0.3 - 0.35\% \times \ln \frac{M}{m} . \quad (24)$$

For a heavy scale in the multi-TeV range, the deviation is about 1%. A determination of the heavy scale to within a factor of 3 requires the precision of the  $\tilde{U}_1$  measurement to be at the  $\sim 0.3\%$  level, which will be taken as our target precision. The effects are clearly smaller than in the SU(2) and SU(3) cases and require correspondingly more precise measurements for similar bounds on the heavy mass scale.

The possibility of measuring  $h_1$  from  $\tilde{e}_R$  production in  $e^+e^-$  collisions at a linear collider has been considered previously in Ref. [20], where bounds from the differential cross section  $d\sigma(e^+e^- \rightarrow \tilde{e}_R^+\tilde{e}_R^-)/d\cos\theta$  were found to imply bounds on  $\tilde{U}_1$  at the  $\sim 1\%$  level. As was pointed out in Ref. [20], such a measurement provides an extremely high precision test of SUSY, and may possibly provide evidence for decoupling effects from heavy sectors. However, as the expected super-oblique corrections in the U(1) sector are small, such a test, as in the chargino case considered in the previous section, is probably not sufficient to determine the heavy superpartner scale to better than an order of magnitude.

To increase this sensitivity, we consider here  $\tilde{e}_R$  pair production in the  $e^-e^-$  mode of a future linear collider. (The extension to  $\tilde{e}_L$  is straightforward and will be discussed at the end of this section.) There are several advantages in considering selectron production at an  $e^-e^-$  collider:

- At an  $e^-e^-$  collider, selectrons are produced only through  $t$ -channel neutralino exchange. The cross section for  $\tilde{e}_R$  production is thus directly proportional to  $h_1^4$ . In contrast, at  $e^+e^-$  colliders, selectrons are produced through both  $s$ - and  $t$ -channel processes. The  $s$ -channel processes are  $h_1$  independent, and may significantly dilute the sensitivity of the cross section observables to variations in  $h_1$ .
- The backgrounds to selectron pair production at  $e^-e^-$  colliders are very small. Most of the major backgrounds present in the  $e^+e^-$  mode are absent; *e.g.*,  $W$  pair and chargino pair production are forbidden by total lepton number conservation. This makes the  $e^-e^-$  environment extremely clean for precision measurements.
- It is possible to highly polarize both  $e^-$  beams. Polarizing both beams right-handed increases the desired  $\tilde{e}_R\tilde{e}_R$  cross section by a factor of 4, and suppresses remaining backgrounds, such as  $e^-\nu W^-$ , even further.

- In order to produce  $\tilde{e}_R^-\tilde{e}_R^-$ , a Majorana mass insertion in the neutralino propagator is needed to flip the chirality. The total cross section therefore increases as the Bino mass  $M_1$  increases as long as  $M_1$  is not too large ( $M_1 \lesssim \sqrt{s}/2$ ). The  $M_1$  dependences of the cross sections for  $e^+e_R^- \rightarrow \tilde{e}_R^+\tilde{e}_R^-$  and  $e_R^-e_R^- \rightarrow \tilde{e}_R^-\tilde{e}_R^-$  are shown in Fig. 8 for  $\sqrt{s} = 500$  GeV and  $m_{\tilde{e}_R} = 150$  GeV. One can see that if  $M_1$  is not too small, the selectron production cross section in the  $e^-e^-$  mode is much larger than in the  $e^+e^-$  mode.<sup>6</sup> This compensates for any reduction in luminosity that may be present in the  $e^-e^-$  mode.
- The  $t$ -channel gaugino mass insertion may also be exploited to reduce theoretical systematic errors arising from uncertainties in the  $\tilde{e}_R$  and  $\tilde{\chi}_1^0$  masses. The  $\tilde{e}_R$  and  $\tilde{\chi}_1^0$  masses are typically constrained from electron energy distribution endpoints. The resulting allowed masses are positively correlated, while the dependence of the total cross section in the  $e^-e^-$  mode on  $m_{\tilde{\chi}_1^0}$  and  $m_{\tilde{e}_R}$  is negatively correlated (in the region of the parameter space in which we are interested). The total cross section may therefore remain approximately constant over the allowed region in the  $(m_{\tilde{e}_R}, m_{\tilde{\chi}_1^0})$  plane. This point will be described in more detail below.

Let us now consider quantitatively the possibility of precisely measuring  $h_1$  using an  $e^-e^-$  collider. We will determine  $h_1$  from the total cross section  $\sigma_R = \sigma(e_R^-e_R^- \rightarrow \tilde{e}_R^-\tilde{e}_R^-)$ . We assume that the  $\tilde{e}_R$  decays directly to  $e\tilde{\chi}_1^0$ , and that  $\tilde{\chi}_1^0$  is the lightest supersymmetric particle and is Bino-like. The cross section is proportional to  $h_1^4$ , so in order to measure  $h_1$  to 0.3%, the cross section must be determined to 1.2%. There are many possible sources of uncertainties, as was mentioned in Sec. III. The experimental statistical and systematic errors will introduce uncertainties in determining  $\sigma_R$  experimentally. Once  $\sigma_R$  is determined, the extraction of  $h_1$  from this measurement depends on many other unknown SUSY parameters and hence suffers from theoretical systematic uncertainties. To achieve the target precision, each source of uncertainty should induce an error in  $\sigma_R$  less than 1%. Of course, if there are several comparable uncertainties, they are required to be even smaller so that their combined error is at the 1% level.

The possible sources of uncertainties in measuring  $\sigma_R$  include:

1. Statistical fluctuation: Fig. 9 shows the total cross section  $\sigma_R$  in the  $(m_{\tilde{e}_R}, M_1)$  plane. We can see that for a significant part of the parameter space ( $M_1$  not too small and  $m_{\tilde{e}_R}$  not too close to threshold), the total cross section is on the order of  $\sim 2000$  fb. Typically only a small fraction of the selectrons are produced along the beam direction ( $< 5\%$  for  $\sin\theta(\tilde{e}_R) < 5^\circ$ ), so most of the events will survive the cuts and be detected. Assuming one year running at luminosity  $\mathcal{L} \sim 20 \text{ fb}^{-1}/\text{yr}$ , we expect  $\sim 40,000$  events, yielding a statistical

---

<sup>6</sup>It is interesting to note that this dependence may allow an alternative high mass scale probe in the Higgsino region where  $|\mu| < M_1, M_2$  and gaugino masses may be very large. If selectron pairs may be produced, their pair-production cross section in the  $e^-e^-$  mode is still substantial and sensitive to  $M_1$  even for very large  $M_1$ , and may be used to determine values of  $M_1$  at the multi-TeV scale. Here, however, we assume that we are in the gaugino region since we are interested in measuring the gaugino couplings.

uncertainty of  $\sim 0.5\%$ . This is further reduced for longer runs, or if an  $e^-e^-$  luminosity comparable to the design  $e^+e^-$  luminosity may be achieved.

2. Backgrounds: Background from electron pair production may be effectively removed by an acoplanarity cut. The major remaining background is then  $e^-\nu W^-$  when followed by  $W^- \rightarrow e^-\nu_e$ , which results from  $e_L^-$  contamination in the  $e_R^-$  polarized beams. The cross section for this background is 400 (43) fb for LL (LR) beam polarization [23]. If both beams are 90% right-polarized, *i.e.*, if only 10% of the electrons in each beam are left-handed, the background is reduced to 12 fb. In principle these backgrounds are calculable and can be subtracted, so the induced uncertainty in  $\sigma_R$  should be negligible.

3. Experimental systematic errors: These include uncertainties in various collider parameters, including the beam energy, luminosity, and so on. Accurate knowledge of the beam polarization is also required. Note, however, that if beam polarization is a dominant source of uncertainty, one may use unpolarized beams instead and run below the  $\tilde{e}_L$  pair production threshold for a longer time to compensate the loss in cross section. The resulting increase in background is acceptable if well-understood. To compare the theoretical cross section and the total number of events, detailed Monte Carlo simulations incorporating effects ranging from initial state radiation and beamstrahlung to detector acceptances must be performed to obtain the predicted number of events passing the cuts. Such simulations are beyond the scope of this paper. We will see, however, that experimental systematic errors are likely to be some of the dominant errors in this analysis, and further studies are necessary.

After obtaining the cross section  $\sigma_R$  from experiment, we need to extract  $h_1$  from  $\sigma_R$ . The associated uncertainties include:

1. Radiative corrections: At the level of precision we are considering, radiative corrections to the cross section must be included. These are required to set the low scale  $m$  so that the heavy scale  $M$  may be inferred from the measured value of  $\tilde{U}_i$ . However, these corrections are calculable, and we expect the uncertainty to be small after the one-loop radiative corrections are included. We have not included such corrections in our calculations.

2. Lepton flavor violation: Until now we have assumed that lepton flavor is conserved, as is approximately true in a wide variety of models. However, if the slepton mass matrices are not diagonalized in the same basis as the lepton mass matrix, the lepton flavor mixing matrix elements will appear at the gaugino vertices. Such mixing may reduce the  $e^-e^-$  selectron pair signal and cause some uncertainties in determining  $h_1$ . However, these lepton flavor violating effects will be well-probed at the same time. For instance, Ref. [24] shows that a mixing angle between the first and second generations of order  $\sin\theta_{12} \sim 0.02$  will be probed at the  $5\sigma$  level. The fractional deviation in the  $e^-e^-$  cross section is at most  $2\sin^2\theta_{12}\cos^2\theta_{12}$ , and so the induced uncertainty in deviation in  $\tilde{U}_1$  is  $\leq \frac{1}{2}\sin^2\theta_{12}\cos^2\theta_{12} \sim 2 \times 10^{-4}$ . If no lepton flavor violation is found, the mixing angles are therefore too small to induce significant uncertainties in  $\tilde{U}_1$ . On the other hand, if lepton flavor violating events are discovered, the total three generation slepton production cross section may be used instead. The backgrounds will then include all 3 generations of leptons from  $W^-$  decay and will be somewhat larger, but from the discussion above, we know that they are small enough at an  $e^-e^-$  collider and can be calculated anyway. Lepton flavor violation therefore should not pose a severe problem, and for simplicity in the remaining discussion, we will assume it is absent.

3. Uncertainties in experimental determination of  $m_{\tilde{e}_R}$  and  $m_{\tilde{\chi}_1^0}$ : These two masses are



the major parameters on which  $\sigma_R$  depends in the gaugino region, and therefore must be known well for a precise prediction of  $\sigma_R$  to be possible. For simplicity, we assume here that  $\tilde{\chi}_1^0$  is pure Bino and  $m_{\tilde{\chi}_1^0} = M_1$ ; the complication of neutralino mixings will be discussed next. The masses  $m_{\tilde{e}_R}$  and  $m_{\tilde{\chi}_1^0}$  can be determined from the energy spectrum of the final state electrons in the  $\tilde{e}_R \rightarrow e\tilde{\chi}_1^0$  decay. The energy distribution is flat for two-body decay with two sharp endpoints determined by  $m_{\tilde{e}_R}$ ,  $m_{\tilde{\chi}_1^0}$ , and  $s$ :

$$E_{\min} = \frac{m_{\tilde{e}_R}}{2} \left( 1 - \frac{m_{\tilde{\chi}_1^0}^2}{m_{\tilde{e}_R}^2} \right) \gamma(1 - \beta), \quad E_{\max} = \frac{m_{\tilde{e}_R}}{2} \left( 1 - \frac{m_{\tilde{\chi}_1^0}^2}{m_{\tilde{e}_R}^2} \right) \gamma(1 + \beta), \quad (25)$$

where

$$\gamma = \frac{\sqrt{s}}{2m_{\tilde{e}_R}}, \quad \beta = \sqrt{1 - \frac{4m_{\tilde{e}_R}^2}{s}}. \quad (26)$$

One can therefore extract  $m_{\tilde{e}_R}$  and  $m_{\tilde{\chi}_1^0}$  from measurements of  $E_{\min}$  and  $E_{\max}$ . As we will see, the uncertainties in  $m_{\tilde{e}_R}$  and  $m_{\tilde{\chi}_1^0}$  are positively-correlated and form a narrow ellipse-like region in the  $(m_{\tilde{e}_R}, m_{\tilde{\chi}_1^0})$  plane. At the same time, the  $t$ -channel mass insertion implies that, while the total cross section  $\sigma_R$  increases as  $m_{\tilde{e}_R}$  decreases, it also increases as  $m_{\tilde{\chi}_1^0}$  increases, and so the constant  $\sigma_R$  contours are approximately parallel to the major axis of the ellipse.

The variation in  $\sigma_R$  on the “uncertainty ellipse” can be very small for some values of  $m_{\tilde{e}_R}$  and  $m_{\tilde{\chi}_1^0}$ . To show this, we assume that  $E_{\min}$  and  $E_{\max}$  are determined independently with uncertainty  $\Delta E$ . The allowed region in the  $(E_{\min}, E_{\max})$  plane is therefore an “uncertainty circle” with radius  $\Delta E$ . This “uncertainty circle” transforms into an “uncertainty ellipse” in the  $(m_{\tilde{e}_R}, m_{\tilde{\chi}_1^0})$  plane, which is shown in Fig. 10 for the central values  $m_{\tilde{e}_R} = 150$  GeV and  $m_{\tilde{\chi}_1^0} = 100$  GeV. The  $\Delta E = 0.5$  GeV and 0.3 GeV ellipses roughly correspond to the  $\Delta\chi^2 = 4.61$  (90% C.L.) and  $\Delta\chi^2 = 2.28$  (68% C.L.) ellipses given in Ref. [6] for a similar analysis with smuon pairs.<sup>7</sup> We also superimpose constant  $\sigma_R$  contours on the same figure. We see that the variation in  $\sigma_R$  induced by uncertainties in  $m_{\tilde{e}_R}$  and  $m_{\tilde{\chi}_1^0}$  is less than 0.3% for  $\Delta E = 0.3$  GeV and this set of the parameters. In Fig. 11, we show the maximal variations in  $\sigma_R$  in the corresponding  $\Delta E = 0.3$  GeV ellipses for different central values of  $m_{\tilde{e}_R}$ ,  $m_{\tilde{\chi}_1^0}$ . For  $m_{\tilde{\chi}_1^0}$  not too small and  $m_{\tilde{e}_R}$  not too close to threshold, there is a large region in the  $(m_{\tilde{e}_R}, m_{\tilde{\chi}_1^0})$  parameter space in which the variation is less than 1%, the target precision. If the variation is too large because  $m_{\tilde{e}_R}$  is too close to threshold, the result can be improved by raising the beam energy, as shown in Fig. 12. The reduction of these theoretical systematic uncertainties is a great advantage for the precision measurement of  $h_1$  at  $e^-e^-$  colliders. In contrast, for  $e^+e^- \rightarrow \tilde{e}_R^+\tilde{e}_R^-$ , the constant cross section contours run roughly perpendicular to the uncertainty ellipse, resulting in a much larger uncertainty.

---

<sup>7</sup>We expect our estimates of endpoint energy uncertainties to be conservative, as they are based on  $e^+e^-$  mode event rates, whereas, given the  $e^-e^-$  cross section, data from the  $e^-e^-$  mode should reduce these errors significantly. The uncertainties are in fact controlled by a number of factors, including total cross section, detector energy resolution, electron energy bin size, and of course, the underlying selectron and neutralino masses. See Ref. [20] for a discussion of this issue.

4. Neutralino mixings: In the discussion so far, we have assumed that the lightest neutralino is pure Bino. This is only true in the limit of  $|\mu| \rightarrow \infty$ . A general neutralino mass matrix depends on the four parameters  $M_1$ ,  $M_2$ ,  $\mu$ , and  $\tan\beta$ . To correctly calculate the cross section, one has to diagonalize the neutralino mass matrix and include contributions from all four neutralino mass eigenstate propagators. Although the dependence of  $\sigma_R$  on  $M_2$ ,  $\mu$ , and  $\tan\beta$  should be weak in the gaugino region, they are not negligible at the required level of precision. To investigate this, we have calculated  $\sigma_R$  for different choices of  $M_1$ ,  $M_2$ ,  $\mu$ , and  $\tan\beta$  while keeping the measurable  $m_{\tilde{\chi}_1^0}$  fixed. By explicit calculation we find that the dependence on  $M_2$  of  $\sigma_R$  is very weak, since  $\tilde{B}$  and  $\tilde{W}_3$  only mix indirectly, and the variation in  $\sigma_R$  is much smaller than 1% for reasonable variations in  $M_2$ . We may therefore assume  $M_2 = 2M_1$  without loss of generality. In Fig. 13 we show the fractional variation of  $\sigma_R$  relative to the pure Bino limit as a function of  $\mu$  and  $\tan\beta$  for fixed  $m_{\tilde{\chi}_1^0} = 100$  GeV and  $m_{\tilde{e}_R} = 150$  GeV. The value of  $M_2 = 2M_1$  is determined by requiring the correct value of  $m_{\tilde{\chi}_1^0}$ . We see that the variation of  $\sigma_R$  is small for large  $|\mu|$  (less than 1% for  $\mu \gtrsim 500$  GeV or  $\mu \lesssim -600$  GeV) but can be up to 2–4% for smaller  $|\mu|$ . Therefore, in order to be able to calculate  $\sigma_R$  at the 1% level, some information about  $\mu$  and  $\tan\beta$  is needed: either a lower bound of  $|\mu| \gtrsim 500 - 600$  GeV is required, or  $\mu$  and  $\tan\beta$  must be bounded to lie within a certain range if the underlying value of  $|\mu|$  is smaller. Such bounds may be obtained from some other processes in different colliders. For example,  $\tilde{\chi}_1^0 \tilde{\chi}_3^0$  production (in  $e^+e^-$  collisions) may probe  $\mu$  up to  $\sqrt{s} - m_{\tilde{\chi}_1^0}$ . Energies of  $\sqrt{s} \sim 1$  TeV, if available, will therefore allow either a determination of  $\mu$  or a sufficiently high lower bound on  $\mu$  for us to obtain a precise prediction of  $\sigma_R$  so that  $h_1$  can be extracted with small uncertainties.

Finally, many of the above considerations apply also to left-handed selectrons. If kinematically accessible, their production cross section  $\sigma_L$  at  $e^-e^-$  colliders may also be used to precisely measure gaugino couplings, since the  $\tilde{e}_L^- \tilde{e}_L^-$  pair production cross section receives contributions from both  $t$ -channel  $\tilde{B}$  and  $\tilde{W}^3$  exchange, and hence depends on both  $h_1$  and  $h_2$ . For equivalent mass selectrons,  $\sigma_L$  is generally even larger than  $\sigma_R$ . Note also that  $\tilde{e}_L$  and  $\tilde{e}_R$  production may be separated either by beam polarization, or, if the selectrons are sufficiently non-degenerate, by kinematics [6] or by running below the higher production thresholds. If the  $\tilde{\chi}_1^\pm$  and  $\tilde{\chi}_2^0$  decay channels are not open, the only decay is  $\tilde{e}_L^- \rightarrow e^- \tilde{\chi}_1^0$  and we will have a large clean sample of events for precision studies. However, in general, the decay patterns may complicate the analysis. The cross section also depends strongly on  $m_{\tilde{\chi}_2^0}$  (in the gaugino region), which could be measured either directly from  $\tilde{\chi}_2^0 \tilde{\chi}_2^0$  production in  $e^+e^-$  collisions, or indirectly by measuring  $M_1$ ,  $M_2$ ,  $\mu$  and  $\tan\beta$  from chargino and  $\tilde{\chi}_1^0$  properties. In the end, a measurement of  $\sigma_L$  bounds a certain combination of  $h_1$  and  $h_2$ . Under the assumption that the heavy particles are fairly degenerate, the deviations  $\tilde{U}_1$  and  $\tilde{U}_2$  are related and determined by the same heavy scale  $M$ , and so  $\sigma_L$  also provides a probe of the heavy scale  $M$ , which, in fact, is generically more sensitive, since  $\tilde{U}_2 > \tilde{U}_1$  in most models. Of course, in the event that both  $\tilde{e}_R$  and  $\tilde{e}_L$  are studied, both  $\tilde{U}_1$  and  $\tilde{U}_2$  may be determined, and we may check that their implications for the heavy scale  $M$  are consistent or find evidence for non-degeneracies in the heavy sector.

In summary, we find that for a fairly general region of the parameter space, selectron production at an  $e^-e^-$  collider may provide an extremely high precision measurement of the gaugino coupling  $h_1$  and super-oblique parameter  $\tilde{U}_1$ . We have investigated both experimental statistical and theoretical systematic uncertainties. By exploiting many appealing

features of the  $e^-e^-$  mode, most uncertainties may be reduced to below 1% in the cross section measurement. The dominant theoretical systematic uncertainty appears to be from neutralino mixings, but even these may be reduced below the 1% level with information from other processes. The remaining uncertainties are experimental systematic uncertainties. These include, for example, the luminosity uncertainty, which has been estimated to be  $\sim 1\%$  [6]. Such issues require further study. Nevertheless, the  $e^-e^-$  mode certainly appears more promising than the  $e^+e^-$  mode. If such errors may be reduced to the 1% level, a precision measurement of  $\tilde{U}_1$  at the level of 0.3% will be possible, providing not only a stringent test of SUSY, but also allowing us to bound the mass scale of the heavy sector to within a factor of 3, even if they are beyond the reach of the LHC. Such a stringent bound would provide strong constraints for model-building, and, in the most optimal case, would provide a target for sparticle searches at even higher energy colliders.

## VI. PROBE OF SU(3) COUPLINGS FROM SQUARKS

In this section, we consider the possibility of probing the heavy superparticle mass scale through their effects on SU(3) gluon and gluino couplings. Such probes require that strongly-interacting sparticles be accessible. Such is the case in the 2–1 models discussed in Sec. I, and these are the scenarios we will consider here. The most relevant decoupling parameters for our study below will be  $\tilde{U}_{32}$  and  $\tilde{U}_{31}$ . In 2–1 models,

$$\tilde{U}_{32(31)} = \frac{h_3/h_{2(1)}}{g_3/g_{2(1)}} - 1 \approx 1.8\%(2.2\%) \times \ln \frac{M}{m} . \quad (27)$$

For heavy superpartners at  $M \sim \mathcal{O}(10 \text{ TeV})$ , these corrections can be as large as  $\sim 10\%$ , much larger than for the corresponding SU(2) and U(1) couplings, and so are promising to investigate.

In 2–1 models, the gluino and third generation sfermions are light, but all other sfermions are heavy. SU(3) effects may then be measured in processes involving gluinos and the bottom and top squarks. At  $e^+e^-$  colliders, squarks may be pair-produced in large numbers [25,26]. However, squark pair production takes place only through  $s$ -channel  $\gamma$  and  $Z$  processes, and so is independent of  $h_i$ . To find cross sections that do depend on  $h_3$ , one may turn to three-body processes, such as  $b\tilde{b}\tilde{g}$  and  $t\tilde{t}\tilde{g}$ , as was noted in Sec. II. In this section, however, we will focus on another possibility and consider measurements of  $h_3$  through squark decay branching ratios.

Any of the  $\tilde{b}_{L,R}$  and  $\tilde{t}_{L,R}$  squarks may be used as a probe. However, the decay paths and backgrounds vary greatly depending on the particular mass patterns of these squarks and the gluino. The boundary conditions for the light sparticle masses are not in general universal, and this is in fact the underlying motivation for the 2–1 framework. The low-energy spectrum may therefore be arbitrary, although, of course, the  $\tilde{t}_L$  and  $\tilde{b}_L$  masses are still related by SU(2) invariance. For concreteness, we will primarily focus on  $\tilde{b}_L$  decays. As will be described below, our analysis will rely only on the number of events with 3 or more tagged  $b$  jets. For simplicity, we will assume that the contributions of other third generation squarks to such events are negligible. This is the case either if these squarks are too heavy to be produced, or if their masses are such that their decays to gluinos are

closed or highly phase-space suppressed. (Note that top squark decays to gluinos are also suppressed by the large top quark mass.) We also take the left-right mixing in the  $\tilde{b}$  sector to be negligible. Such an assumption may be tested by measurements of the  $\tilde{b}_L$  properties themselves [26], or, for example, by measurements of  $\tan\beta$  from other sectors [27]. Finally, we assume that the lighter neutralinos and chargino are well-studied and are determined to be highly gaugino-like by, for example, directly measuring or placing lower bounds on Higgsino masses.<sup>8</sup>

As individual decay widths are difficult to measure, our analysis will depend on measuring branching ratios, and is only possible when two or more decay modes are open. As we are interested in the SU(3) gaugino coupling  $h_3$  in this section, we assume  $m_{\tilde{g}} + m_b < m_{\tilde{b}_L}$  so that the gluino decay mode is open. (Of course, if the gluino decay mode is closed but both Wino and Bino decay modes are open, a measurement of  $h_2/h_1$  from these branching ratios may also be used to probe decoupling effects.) The branching ratios then depend on  $h_3/h_2$  and  $h_3/h_1$  and probe the decoupling parameters  $\tilde{U}_{32(31)}$  given above.

The two-body decay widths of  $\tilde{b}_L$  to  $\tilde{g}$ ,  $\tilde{\chi}_1^\pm$ ,  $\tilde{\chi}_2^0$ , and  $\tilde{\chi}_1^0$  (assuming that  $\tilde{\chi}_1^\pm$ ,  $\tilde{\chi}_2^0$ , and  $\tilde{\chi}_1^0$  are pure gauginos) are

$$\begin{aligned}\Gamma(\tilde{b}_L \rightarrow b\tilde{g}) &= \frac{4}{3} \frac{h_3^2}{8\pi} m_{\tilde{b}_L} P(m_{\tilde{b}_L}, m_{\tilde{g}}, m_b) \equiv \frac{h_3^2}{8\pi} m_{\tilde{b}_L} P_3, \\ \Gamma(\tilde{b}_L \rightarrow b\tilde{\chi}_2^0) &= \frac{1}{4} \frac{h_2^2}{8\pi} m_{\tilde{b}_L} P(m_{\tilde{b}_L}, m_{\tilde{\chi}_2^0}, m_b) \equiv \frac{h_2^2}{8\pi} m_{\tilde{b}_L} P_2, \\ \Gamma(\tilde{b}_L \rightarrow t\tilde{\chi}_1^\pm) &= \frac{1}{2} \frac{h_2^2}{8\pi} m_{\tilde{b}_L} P(m_{\tilde{b}_L}, m_{\tilde{\chi}_1^\pm}, m_t) \equiv \frac{h_2^2}{8\pi} m_{\tilde{b}_L} P_2', \\ \Gamma(\tilde{b}_L \rightarrow b\tilde{\chi}_1^0) &= \frac{1}{36} \frac{h_1^2}{8\pi} m_{\tilde{b}_L} P(m_{\tilde{b}_L}, m_{\tilde{\chi}_1^0}, m_b) \equiv \frac{h_1^2}{8\pi} m_{\tilde{b}_L} P_1,\end{aligned}\tag{28}$$

where these equations define  $P_3$ ,  $P_2$ ,  $P_2'$ , and  $P_1$ , and

$$\begin{aligned}P(m_0, m_1, m_2) &= \theta(m_0 - m_1 - m_2) \left\{ \left( 1 - \frac{m_1^2 + m_2^2}{m_0^2} \right) \sqrt{\left( \frac{1}{2} - \frac{m_1^2}{2m_0^2} + \frac{m_2^2}{2m_0^2} \right)^2 - \frac{m_2^2}{m_0^2}} \right. \\ &\quad \left. + 2 \left[ \left( \frac{1}{2} - \frac{m_1^2}{2m_0^2} + \frac{m_2^2}{2m_0^2} \right)^2 - \frac{m_2^2}{m_0^2} \right] \right\}\end{aligned}\tag{29}$$

is the phase space factor for a scalar particle of mass  $m_0$  decaying into two fermions with masses  $m_1$  and  $m_2$ . The branching ratio for  $\tilde{b}_L \rightarrow b\tilde{g}$  is then given by

$$B_{\tilde{g}} = B(\tilde{b}_L \rightarrow b\tilde{g}) = \frac{D_{32}^2 P_3}{D_{12}^2 P_1 + P_2 + P_2' + D_{32}^2 P_3},\tag{30}$$

where  $D_{ij} \equiv h_i/h_j = (1 + \tilde{U}_{ij})g_i/g_j$ .

---

<sup>8</sup>If, however, the Higgsinos are in the heavy sector, significant non-decoupling contributions to the gaugino couplings from the large third generation Yukawa couplings must be included [13].

The deviation of  $D_{12} = h_1/h_2$  from  $g_1/g_2$  is much smaller than that of  $D_{32}$  from  $g_3/g_2$ , and the term involving  $D_{12}$  is suppressed by the small  $U(1)$  coupling, so it is a good approximation to fix  $D_{12} = g_1/g_2$ . If the gluino branching fraction can be measured, and all the relevant particle masses are known, then from Eq. (30) we can obtain  $D_{32}$ :

$$D_{32} = \left[ \frac{D_{12}^2 P_1 + P_2 + P_2'}{P_3} \frac{B_{\tilde{g}}}{1 - B_{\tilde{g}}} \right]^{\frac{1}{2}}. \quad (31)$$

Combining this with the measured value of  $g_3/g_2$ <sup>9</sup>, we then have a measurement of  $\tilde{U}_{32}$  and a constraint on the heavy sector mass scale. Of course, as in the previous sections, such a measurement is subject to a number of uncertainties. Uncertainties in the measurement of  $B_{\tilde{g}}$  arise from statistical fluctuations, backgrounds, and experimental systematic errors, while the extraction of  $D_{32}$  from  $B_{\tilde{g}}$  is subject to theoretical systematic uncertainties from imprecisely known SUSY parameters. We will discuss the theoretical systematic uncertainties first.

The major theoretical systematic uncertainties are the uncertainties in  $m_{\tilde{b}_L}$  and  $m_{\tilde{g}}$ . For all measurement methods, these masses enter the determination of  $D_{32}$  through the phase space factors in Eq. (31). In addition, depending on the method used to measure  $B_{\tilde{g}}$ , a dependence on  $m_{\tilde{b}_L}$  may also enter through this quantity. This is the case, for example, if  $B_{\tilde{g}}$  is determined by comparing the number of events in a particular channel to the total  $\tilde{b}_L \bar{b}_L$  cross section, and this total cross section is determined theoretically by its dependence on  $m_{\tilde{b}_L}$ . However, the uncertainties entering from the dependence of  $B_{\tilde{g}}$  on  $m_{\tilde{b}_L}$ , in addition to being method-dependent, are typically negligible relative to other errors. For example, for the method just described, we have found that for  $m_{\tilde{b}_L}$  significantly below threshold, the uncertainty from the dependence of  $B_{\tilde{g}}$  on  $m_{\tilde{b}_L}$  is small compared to that from the phase space factors. This is no longer the case for  $m_{\tilde{b}_L}$  near threshold, as there the total cross section is sensitive to  $m_{\tilde{b}_L}$ , but in this region, the cross section is small and statistical uncertainties are dominant.

We therefore consider only the theoretical systematic uncertainties from the phase space factors. The fractional uncertainties in  $D_{32}$ , or equivalently, the uncertainties in  $\tilde{U}_{32}$ , from  $m_{\tilde{b}_L}$  and  $m_{\tilde{g}}$  systematic errors are given by

$$\frac{d\tilde{U}_{32}}{dm_{\tilde{b}_L}} \approx \frac{1}{D_{32}} \frac{dD_{32}}{dm_{\tilde{b}_L}} = \frac{1}{2(D_{12}^2 P_1 + P_2 + P_2')} \left( D_{12}^2 \frac{\partial P_1}{\partial m_{\tilde{b}_L}} + \frac{\partial P_2}{\partial m_{\tilde{b}_L}} + \frac{\partial P_2'}{\partial m_{\tilde{b}_L}} \right) - \frac{1}{2P_3} \frac{\partial P_3}{\partial m_{\tilde{b}_L}} \quad (32)$$

$$\frac{d\tilde{U}_{32}}{dm_{\tilde{g}}} \approx \frac{1}{D_{32}} \frac{dD_{32}}{dm_{\tilde{g}}} = -\frac{1}{2P_3} \frac{\partial P_3}{\partial m_{\tilde{g}}}. \quad (33)$$

We plot the systematic errors from  $m_{\tilde{b}_L}$  and  $m_{\tilde{g}}$  in Figs. 14 and 15, respectively. The uncertainties in  $\tilde{U}_{32}$  are in percent per GeV variation in  $m_{\tilde{b}_L}$  or  $m_{\tilde{g}}$  and are plotted in the  $(m_{\tilde{b}_L}, m_{\tilde{b}_L} - m_{\tilde{g}})$  plane. Motivated by the current bounds on squark masses and the prejudice

---

<sup>9</sup>Assuming that the  $\mathcal{O}(\alpha_s^3)$  perturbative QCD corrections are calculated, the uncertainty in  $\alpha_s(m_Z^2)$  from  $q\bar{q}$  events at the NLC is estimated to be at the 1% level [7] and is therefore negligible for this study.

that colored superparticles should be heavier than uncolored ones, we have taken a value of  $\sqrt{s} = 1$  TeV such that we may pair produce squarks with masses of up to 500 GeV. (Note that some regions of the plane are for gluino masses that have already been excluded by current bounds.) At each point, we have assumed that the underlying parameters are given by the gaugino mass unification relations  $m_{\tilde{g}} = 3.3m_{\tilde{\chi}_2^0} = 3.3m_{\tilde{\chi}_1^\pm} = 6.6m_{\tilde{\chi}_1^0}$ . (The abrupt behavior of the contours in Fig. 14 results from the opening of the decay  $\tilde{b}_L \rightarrow t\tilde{\chi}_1^\pm$ .) For decreasing  $m_{\tilde{b}_L} - m_{\tilde{g}}$ , the uncertainties increase, as the phase space for decays to gluinos shrinks and the decay width to gluinos becomes more sensitive to  $m_{\tilde{b}_L}$  and  $m_{\tilde{g}}$ . The theoretical systematic uncertainty in  $\tilde{U}_{32}$  is therefore highly dependent on the mass splitting  $m_{\tilde{b}_L} - m_{\tilde{g}}$ . We see generally, however, that for this uncertainty to be below 10%,  $m_{\tilde{b}_L}$  and  $m_{\tilde{g}}$  typically must be measured to within a few GeV. Measurements of squark masses at this level have been shown to be possible at the NLC, even in the presence of cascade decays [25]. Gluino masses may be measured at the NLC in the scenarios we are considering through squark decays to gluinos. Alternatively, it is possible that the mass difference  $m_{\tilde{b}_L} - m_{\tilde{g}}$  could be measured at the LHC through methods similar to those described in Ref. [4]. However, estimates of the gluino mass resolution certainly merit further investigation.

The phase space factors also depend on other mass parameters as well, such as  $m_{\tilde{\chi}_{1,2}^0}$  and  $m_{\tilde{\chi}_1^\pm}$ , so there are also uncertainties induced by these unknown masses. However, these masses are expected to be much smaller than  $m_{\tilde{b}_L}$  and  $m_{\tilde{g}}$ . The phase space factors are therefore larger for  $\tilde{b}_L$  decays into these particles and are less sensitive to their masses. In addition, these masses will probably be known more precisely than  $m_{\tilde{b}_L}$  and  $m_{\tilde{g}}$ . We therefore expect the uncertainties coming from these other masses to be much smaller than those from  $m_{\tilde{b}_L}$  and  $m_{\tilde{g}}$ .

In the above discussion, we assume that the lighter neutralinos and charginos are pure gauginos. As discussed in the previous sections, neutralino and chargino mixings may also introduce some uncertainties in determining the gaugino couplings. However, here the non-decoupling effects we expect are much larger ( $\sim 10\%$  versus  $\sim 1 - 3\%$  in previous cases). The uncertainties from these mixings, while possibly significant for the previous cases, are expected to be small relative to the 10% corrections possible in the SU(3) couplings.

We now consider the experimental statistical and systematic errors arising in the measurement of  $B_{\tilde{g}}$ . To measure this branching fraction, we will exploit the fact that gluino decays tend to give more  $b$  quarks in the final state than do decays to the electroweak gauginos. Decays to the Bino and Winos produce one  $b$  quark. Decays to gluinos are followed by gluino decays, which in 2-1 models are dominated by decays through off-shell  $t$ - and  $b$ -squarks, resulting in an additional two  $b$  quarks in the final state.<sup>10</sup> Thus,  $\tilde{b}_L\tilde{b}_L$  pair events with 0, 1, and 2 gluino decays result in 2, 4, and 6  $b$  quarks, respectively.

At the NLC, excellent  $b$ -tagging efficiencies and purities are expected. We will take

---

<sup>10</sup>In fact, additional  $b$  quarks may appear in both Wino and gluino decay modes if neutralinos  $\tilde{\chi}_2^0$  are produced that then decay via  $\tilde{\chi}_2^0 \rightarrow b\bar{b}\tilde{\chi}_1^0$ . We will assume that this  $\tilde{\chi}_2^0$  branching fraction is well-measured. For simplicity, in the quantitative results presented below, we assume that  $\tilde{\chi}_2^0$  decays to  $b$  quarks are absent, as would be the case, for example, if the two-body decay  $\tilde{\chi}_2^0 \rightarrow \tau\tau$  is open.

the probability of tagging a  $b$  ( $c$ ) quark as a  $b$  quark to be  $\epsilon_b = 60\%$  ( $\epsilon_c = 2.6\%$ ), with a negligible probability for light quarks [28]. We also make the crude assumption that the probability of tagging multi- $b$  events is given simply by combinatorics, so that the probability of tagging  $m$  of  $n$   $b$  jets is  $\binom{n}{m} \epsilon_b^m (1 - \epsilon_b)^{n-m}$ . With these assumptions, we may bound the gluino branching fraction by measuring  $N_i$ , the number of events with  $i = 3, 4, 5$  tagged  $b$  jets, along with the total cross section determined by  $m_{\tilde{b}_L}$ , which we assume is measured by kinematical arguments [25]. (We may also use other channels; however,  $N_2$  receives huge backgrounds from  $t\bar{t}$  production, and the number of events with 6 tagged  $b$  jets is not statistically significant.) The standard model backgrounds to multi- $b$  events include  $t\bar{t}$ ,  $t\bar{t}Z$ ,  $ZZZ$ ,  $\nu\bar{\nu}ZZ$ , and  $t\bar{t}h$  [29]. At 1 TeV, the resulting backgrounds with 3, 4, and 5 tagged  $b$  jets, after including all branching fractions and the tagging efficiencies given above, were calculated in Ref. [27] and found to be 4.0 fb, 1.0 fb, and 0.0095 fb, respectively. In our calculations we include only standard model backgrounds. Additional multi- $b$  events may arise from other SUSY processes, such as  $\tilde{t}\bar{\tilde{t}}$  production followed by decays  $\tilde{t} \rightarrow t\tilde{g}$ . Such squark processes also are dependent on the super-oblique parameters, however, and so may be included as signal. The analysis will be more complicated and will not be considered here.

We would now like to determine quantitatively what bounds on deviations in  $\tilde{U}_{32}$  may be set by measurements of  $N_i$ . We will take a central value of  $\tilde{U}_{32} = 0$ ; we expect the errors to be uniform for other central values. We define a simple  $\Delta\chi^2$  variable

$$\Delta\chi^2 \equiv \sum_{i=3}^5 \frac{(N_i - N'_i)^2}{N'_i}, \quad (34)$$

where  $N_i$  is the sum of the number of signal and background events with  $i$  tagged  $b$  jets assuming  $\tilde{U}_{32} = 0$ , and  $N'_i$  is the similar quantity for a postulated  $\tilde{U}'_{32}$ . For given underlying parameters  $\sqrt{s}$ ,  $m_{\tilde{b}_L}$ ,  $m_{\tilde{g}}$  and integrated luminosity  $L$ , the values of  $\tilde{U}'_{32}$  yielding  $\Delta\chi^2 = 1$  (68% C.L.) then give the statistical uncertainty. The fractional error in  $\tilde{U}_{32}$  from such statistical uncertainties for  $\sqrt{s} = 1$  TeV and (unpolarized) integrated luminosity  $L = 200 \text{ fb}^{-1}$  is given Fig. 16. The statistical uncertainties grow rapidly as  $m_{\tilde{b}_L}$  approaches its threshold limit of 500 GeV, as expected. The statistical uncertainty, however, also depends on the mass difference  $m_{\tilde{b}_L} - m_{\tilde{g}}$ . For optimal mass splittings, the gluino decay is fairly phase space-suppressed, yielding roughly an equal number of gluino and Wino decays. The number of events in the different channels  $N_i$  is then highly sensitive to variations in  $\tilde{U}_{32}$ . However, for large or very small mass splittings, either the gluino or the Wino decay dominates, in which case sensitivity to  $\tilde{U}_{32}$  is weak.

The total error receives contributions from all three of the sources shown in Figs. 14–16. We see that if  $\tilde{b}_L$  squarks are produced significantly above threshold, the  $\tilde{b}_L$  and gluino masses are measured to a few GeV, and the squark-gluino mass splittings are moderate, in the range  $25 \text{ GeV} \lesssim m_{\tilde{b}_L} - m_{\tilde{g}} \lesssim 100 \text{ GeV}$ , the combined uncertainty is below the  $\sim 10\%$  level. For nearly ideal mass splittings, the uncertainties can be much below this level, possibly yielding a precise measurement of the heavy sector scale. Note, however, that possibly large experimental systematic errors have not been included. For this study, a particular source of concern is the  $b$  tagging efficiency for multi- $b$  events, which must be well-understood for an accurate measurement to be possible.

Before concluding, we consider briefly the possibility of measuring the super-oblique

parameters through  $\tilde{b}_R$  branching ratios. In this case, the Wino decays are closed, and so only the gluino and Bino modes compete. We find that the strongest bounds on  $\tilde{U}_{31}$  come from the observation of squark pair events in which both squarks decay directly to Binors. Such decays yield clean events with only two acoplanar  $b$  jets, and may be isolated from standard model backgrounds with simple cuts [30]. In Ref. [25], such cuts were found to yield efficiencies of 60–80% for squark pair events. By measuring the number of double direct Bino decays, and again determining the total cross section by measuring  $m_{\tilde{b}_R}$  kinematically, bounds on  $\tilde{U}_{31}$  may be found. In Fig. 17, the statistical uncertainties from such a determination are given. Not surprisingly, we find that in this case, a large phase space suppression of the gluino mode is required to enhance the number of double Bino decay events. A statistical uncertainty at the level of  $\sim 10\%$  is achievable only for  $m_{\tilde{b}_R} - m_{\tilde{g}} \lesssim 30$  GeV. Of course, one may also include data from multi- $b$  events as in the previous case, but such considerations do not improve the results noticeably.

## VII. CONCLUSIONS

If some of the superpartners of the standard model particles are heavy and beyond the reach of planned future colliders, we must rely on indirect methods to study them before their discovery. Such heavy superpartners decouple from most experimentally accessible processes. However, heavy superpartner masses break supersymmetry, and so violate the SUSY relations  $g_i = h_i$  between gauge boson and gaugino couplings at scales below the heavy superpartner mass scale  $M$ . Deviations from these relations are most conveniently parametrized in terms of the super-oblique parameters  $\tilde{U}_i$  [13] and increase logarithmically with  $M$ . Therefore, precision measurements of the gaugino couplings  $h_i$  in processes involving the light superpartners will provide important (and possibly the only) probes of the heavy superpartner sector for the foreseeable future.

There are many low energy processes and observables involving the light superpartners and gauginos that depend on the gaugino couplings  $h_i$  and therefore may serve as probes of the super-oblique parameters. These were systematically classified in Sec. II. However, in practice, these observables are subject to many systematic and statistical uncertainties, and not all of them can be measured to the required precision to provide significant bounds on the heavy sector. In this paper, we studied three promising examples at proposed linear  $e^\pm e^-$  colliders, one for each of the three coupling constant relations using three different superparticles processes. We exploited the versatility of planned linear colliders, such as their highly polarized beams, tunable beam energy, and the  $e^-e^-$  option, to improve the precision of the measurements.

In the first example, chargino pair production in  $e^+e^-$  collisions was used to study the SU(2) gaugino coupling  $h_2$ . From the total cross section, the truncated forward-backward asymmetry, and a precisely measured sneutrino mass  $m_{\tilde{\nu}_e}$ , measurements of the super-oblique parameter  $\tilde{U}_2$  at the level of  $\sim 2 - 3\%$  are possible. We demonstrated the importance of being able to choose an optimal beam energy so that the experimental observables are most sensitive to  $\tilde{U}_2$ . Note that, since we expect greater deviations in the SU(2) relation than the U(1) relation, such results provide bounds on the heavy scale  $M$  that are roughly equivalent to those previously achieved with  $\tilde{e}_R$  pair production at  $e^+e^-$  colliders [20].



In the second example, we considered a measurement of  $h_1$  from  $\tilde{e}_R^- \tilde{e}_R^-$  production at an  $e^- e^-$  collider. Such colliders allow measurements that are extremely clean both experimentally and theoretically, and therefore provide an excellent environment for precision studies. Such measurements also suffer less from uncertainties in the relevant SUSY parameters. If the experimental systematic uncertainties are under control,  $\tilde{U}_1$  may be measured to  $\sim 0.3\%$  for a wide range of the parameter space. Such a high precision measurement may provide a determination of the heavy scale within a factor of 3, which is a striking improvement over the  $e^+ e^-$  results described above.

The last observables we considered were branching ratios of bottom squarks decay into gluinos and other gauginos. These decays can be used to measure the ratios of gaugino couplings  $h_3/h_2$  and  $h_3/h_1$ . Although larger uncertainties are usually associated with strongly-interacting particles, the deviation from the SUSY relation  $h_3 = g_3$  is also expected to be larger. We find that, for squark production significantly above threshold and small to moderate squark-gluino mass splittings, it is possible to obtain a measurement of  $\tilde{U}_{32}$  which is sensitive to deviations from the SUSY relation.

These examples imply that the prospects for precision measurements of gaugino couplings in different scenarios are indeed promising. We have studied various possible uncertainties in these measurements and find that most of them may be controlled (at least in some region of the parameter space), though a complete understanding of all uncertainties would require detailed experimental simulations that are beyond the scope of this study. For this study, it is crucial that collider parameters be well understood and precisely measured. Further experimental studies on these issues are strongly encouraged.

The implications of measurements of the super-oblique parameters depend strongly on what scenario is realized in nature. If some number of superpartners are not yet discovered, bounds on the super-oblique parameters may lead to bounds on the mass scale of the heavy particles. In addition, if measurements of more than one super-oblique parameter may be made, some understanding of the relative splittings in the heavy sector may be gained. Inconsistencies among the measured values of the different super-oblique parameters could also point to additional inaccessible exotic particles with highly split multiplets that are not in complete representations of a grand-unified group. In addition, negative values of the parameters will imply new strong Yukawa interactions involving the SM fields [13].

If, on the other hand, all superpartners of the standard model particles are found, the consistency of all super-oblique parameters with zero will be an important check of the supersymmetric model with minimal field content. If instead deviations of the super-oblique parameters from zero are found, such measurements will provide exciting evidence for new exotic sectors with highly split multiplets not far from the weak scale [13]. These insights could also play an important role in evaluating future proposals for colliders with even higher energies, such as the muon collider or higher energy hadron machines.

In summary, if supersymmetry is discovered, the super-oblique parameters may allow powerful constraints from precision measurements on otherwise inaccessible physics. Their measurement may also have wide implications for theories beyond the minimal supersymmetric standard model, just as the oblique corrections of the standard model provide strong constraints on technicolor models and other extensions of the standard model.

## ACKNOWLEDGMENTS

The authors are grateful to M. Peskin and X. Tata for conversations. This work was supported in part by the Director, Office of Energy Research, Office of High Energy and Nuclear Physics, Division of High Energy Physics of the U.S. Department of Energy under Contracts DE-AC03-76SF00098 and DE-AC02-76CH03000, and in part by the NSF under grants PHY-95-14797 and PHY-94-23002. J.L.F. is supported by a Miller Institute Research Fellowship and thanks the high energy theory group at Rutgers University for its hospitality.

While completing this work, we learned of related work in progress [31]. We thank D. Pierce, L. Randall, and S. Thomas for conversations and for bringing this work to our attention.

## REFERENCES

- [1] J. Ellis, K. Enqvist, D. V. Nanopoulos, and F. Zwirner, *Mod. Phys. Lett. A* **1**, 57 (1986); R. Barbieri and G. F. Giudice, *Nucl. Phys. B* **306**, 63 (1988); G. W. Anderson and D. J. Castano, *Phys. Lett. B*, **347**, 300 (1995); *ibid.*, *Phys. Rev. D* **52**, 1693 (1995); *ibid.*, *Phys. Rev. D* **53**, 2403 (1996).
- [2] CMS Collaboration, Technical Proposal, CERN/LHCC/94-38 (1994); ATLAS Collaboration, Technical Proposal, CERN/LHCC/94-43 (1994).
- [3] The SUSY Working Group, J. Bagger *et al.*, in *Proceedings of the 1996 DPF/DPB Summer Study on New Directions for High Energy Physics (Snowmass '96)*, Colorado, June 25 – July 12, 1996, hep-ph/9612359.
- [4] The LHC SUSY Subgroup, A. Bartl *et al.*, in *Proceedings of the 1996 DPF/DPB Summer Study on New Directions for High Energy Physics (Snowmass '96)*, Colorado, June 25 – July 12, 1996, LBNL-39413; I. Hinchliffe, F. E. Paige, M. D. Shapiro, J. Söderqvist, and W. Yao, LBNL-39412, hep-ph/9610544.
- [5] H. Baer, C.-h. Chen, F. Paige, and X. Tata, *Phys. Rev. D* **52**, 2746 (1995); *ibid.*, **53**, 6241 (1996).
- [6] JLC Group, *JLC-I*, KEK Report No. 92-16, Tsukuba (1992); T. Tsukamoto, K. Fujii, H. Murayama, M. Yamaguchi, and Y. Okada, *Phys. Rev. D* **51**, 3153 (1995).
- [7] NLC ZDR Design Group and the NLC Physics Working Group, S. Kuhlman *et al.*, *Physics and Technology of the Next Linear Collider*, hep-ex/9605011; The NLC Design Group, C. Adolphsen *et al.*, *Zeroth-Order Design Report for the Next Linear Collider*, LBNL-PUB-5424, SLAC Report No. 474, UCRL-ID-124161 (1996).
- [8] ECFA/DESY LC Physics Working Group, E. Accomando *et al.*, DESY-97-100, hep-ph/9705442.
- [9] H. Murayama and M. E. Peskin, *Ann. Rev. Nucl. Part. Sci.* **46**, 533 (1996), hep-ex/9606003.
- [10] The NLC SUSY Subgroup, M. N. Danielson *et al.*, in *Proceedings of the 1996 DPF/DPB Summer Study on New Directions for High Energy Physics (Snowmass '96)*, Colorado, June 25 – July 12, 1996.
- [11] M. Peskin and T. Takeuchi, *Phys. Rev. Lett.* **65**, 964 (1990); *ibid.*, *Phys. Rev. D* **46**, 381 (1992).
- [12] B. Holdom and J. Terning, *Phys. Lett. B* **247**, 88 (1990); M. Golden and L. Randall, *Nucl. Phys. B* **361**, 3 (1991); G. Altarelli and R. Barbieri, *Phys. Lett. B* **253**, 161 (1991); G. Altarelli, R. Barbieri, and S. Jadach, *Nucl. Phys. B* **269**, 3 (1992).
- [13] H.-C. Cheng, J. L. Feng, and N. Polonsky, FERMILAB-PUB-97/177-T, LBNL-40465, UCB-PTH-97/33, RU-97-45, hep-ph/9706438.
- [14] L. Randall, talk presented at Supersymmetry 97, Fifth International Conference on Supersymmetries in Physics, The University of Pennsylvania, Philadelphia, May 27–31, 1997.
- [15] A. B. Lahanas and D. V. Nanopoulos, *Phys. Rept.* **145**, 1 (1987).
- [16] M. Dine, W. Fischler, and M. Srednicki, *Nucl. Phys. B* **189**, 575 (1981); C. Nappi and B. Ovrut, *Phys. Lett. B* **113**, 175 (1982); M. Dine and W. Fischler, *Nucl. Phys. B* **204**, 346 (1982); L. Alvarez-Gaume, M. Claudson and M. Wise, *Nucl. Phys. B* **207**, 96 (1982); M. Dine, A. Nelson, and Y. Shirman, *Phys. Rev. D* **51**, 1362 (1995); M. Dine, A. Nelson, Y. Nir, and Y. Shirman, *Phys. Rev. D* **53**, 2658 (1996).

- [17] N. Arkani-Hamed, H.-C. Cheng, and T. Moroi, Phys. Lett. B **387**, 529 (1996).
- [18] S. Dimopoulos and G. F. Giudice, Phys. Lett. B **357**, 573 (1995); A. Pomarol and D. Tommasini, Nucl. Phys. **B466**, 3 (1996); G. Dvali and A. Pomarol, Phys. Rev. Lett. **77**, 3728 (1996); A. G. Cohen, D. B. Kaplan, and A. E. Nelson, Phys. Lett. B **388**, 588 (1996); A. G. Cohen, D. B. Kaplan, F. Lepeintre, and A. E. Nelson, Phys. Rev. Lett. **78**, 2300 (1997); R. N. Mohapatra and A. Riotto, Phys. Rev. D **55**, 1 (1997); R.-J. Zhang, JHU-TIPAC-97004, hep-ph/9702333; A. E. Nelson and D. Wright, UW/PT-97-03, hep-ph/9702359; H. P. Nilles and N. Polonsky, RU-97-47; N. Polonsky, talk presented at Supersymmetry 97, Fifth International Conference on Supersymmetries in Physics, The University of Pennsylvania, Philadelphia, May 27-31, 1997; A. E. Nelson, talk presented at Supersymmetry 97, Fifth International Conference on Supersymmetries in Physics, The University of Pennsylvania, Philadelphia, May 27-31, 1997.
- [19] J. L. Feng, H. Murayama, M. E. Peskin, and X. Tata, Phys. Rev. D **52**, 1418 (1995).
- [20] M. M. Nojiri, K. Fujii, and T. Tsukamoto, Phys. Rev. D **54**, 6756 (1996).
- [21] K. Hikasa and Y. Nakamura, Z. Phys. C **70**, 139 (1996).
- [22] R. Becker and C. Vander Velde, in *Proceedings of the European Meeting of the Working Groups on Physics and Experiments at Linear  $e^+e^-$  Colliders*, ed. P. M. Zerwas, DESY-93-123C, p. 457.
- [23] D. Choudhury, and F. Cuyper, Nucl. Phys. **B429**, 33 (1994).
- [24] N. Arkani-Hamed, H.-C. Cheng, J. L. Feng, and L. J. Hall, Phys. Rev. Lett. **77**, 1937 (1996).
- [25] J. L. Feng and D. E. Finnell, Phys. Rev. D **49**, 2369 (1994).
- [26] A. Bartl, H. Eberl, S. Kraml, W. Majerotto, W. Porod, and A. Sopczak, UWTHPH-1996-66, hep-ph/9701336.
- [27] J. L. Feng and T. Moroi, LBNL-39579, UCB-PTH-96/51, hep-ph/9612333.
- [28] D. Jackson, talk given at Snowmass '96, Colorado, June 25 - July 12, 1996.
- [29] H. Murayama, Ph.D. thesis, UT-580 (1991).
- [30] J.-F. Grivaz, in *Physics and Experiments with Linear Colliders*, Proceedings of the Workshop, Saariselka, Finland, 1991, edited by R. Orava, P. Eerola, and M. Nordberg (World Scientific, River Edge, NJ, 1992), Vol. 1, p. 353.
- [31] E. Katz, L. Randall, and S. Su, MIT-CTP-2646, in preparation; D. Pierce and S. Thomas, SLAC-PUB-7474, SU-ITP 97-24, in preparation; D. Pierce, M. Nojiri, and Y. Yamada, SLAC-PUB-7558, in preparation.

# FIGURES

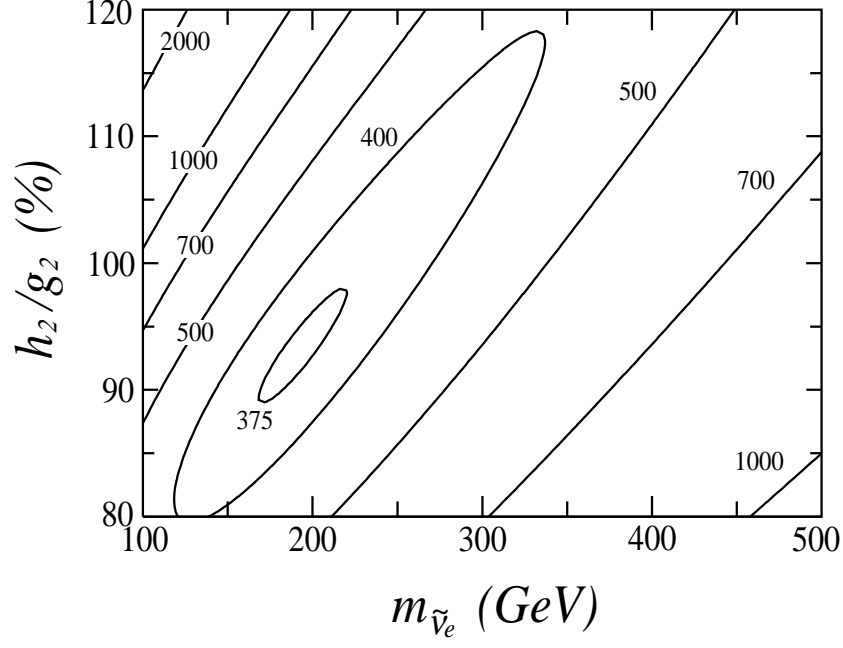


FIG. 1. Contours of constant chargino pair production cross section  $\sigma_L$  in fb in the  $(m_{\tilde{\nu}_e}, h_2)$  plane for underlying parameters  $(\mu, M_2, \tan \beta, M_1/M_2) = (-500 \text{ GeV}, 170 \text{ GeV}, 4, 0.5)$  and  $\sqrt{s} = 500 \text{ GeV}$ .

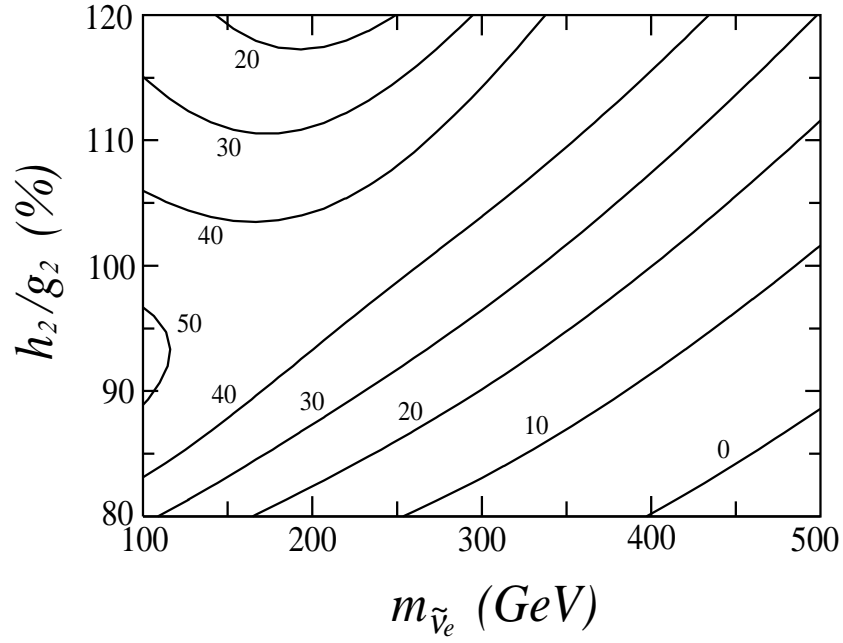


FIG. 2. Contours of constant chargino forward-backward asymmetry  $A_L^\chi$  in percent in the  $(m_{\tilde{\nu}_e}, h_2)$  plane for underlying parameters  $(\mu, M_2, \tan \beta, M_1/M_2) = (-500 \text{ GeV}, 170 \text{ GeV}, 4, 0.5)$  and  $\sqrt{s} = 500 \text{ GeV}$ .

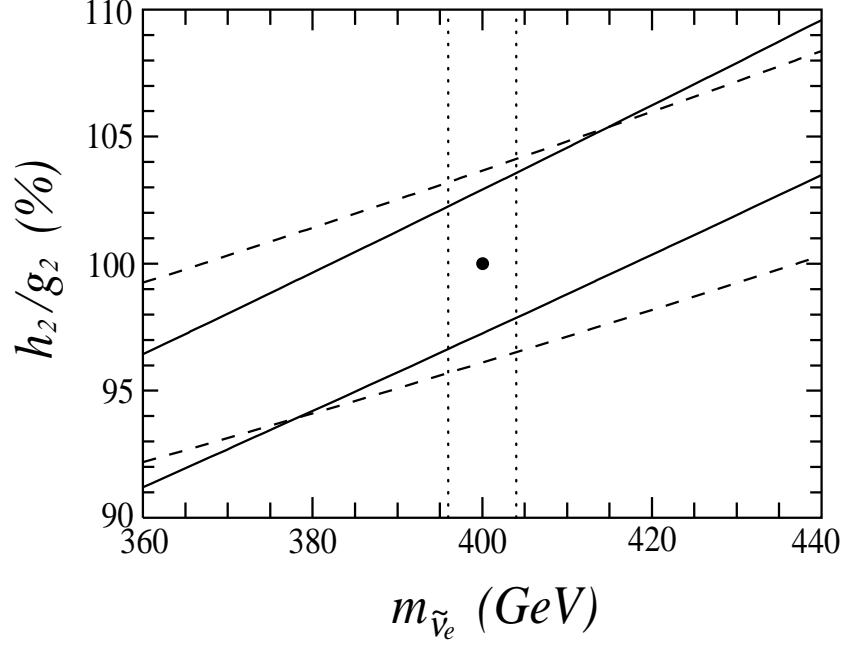


FIG. 3. The allowed region in the  $(m_{\tilde{\nu}_e}, h_2)$  plane for  $\sqrt{s} = 500$  GeV and  $L = 100 \text{ fb}^{-1}$ . The solid (dashed) curves are  $1\sigma$  contours of constant  $\sigma_L(A_L^\chi)$ , and the underlying parameter point  $(\mu, M_2, \tan\beta, M_1/M_2, m_{\tilde{\nu}_e}) = (-500 \text{ GeV}, 170 \text{ GeV}, 4, 0.5, 400 \text{ GeV})$  is indicated. The allowed region is bounded by the  $\sigma_L$  and  $A_L^\chi$  contours and the bound on  $m_{\tilde{\nu}_e}$ ; for reference, the bound  $\Delta m_{\tilde{\nu}_e} = 4 \text{ GeV}$  is given by the dotted contours.

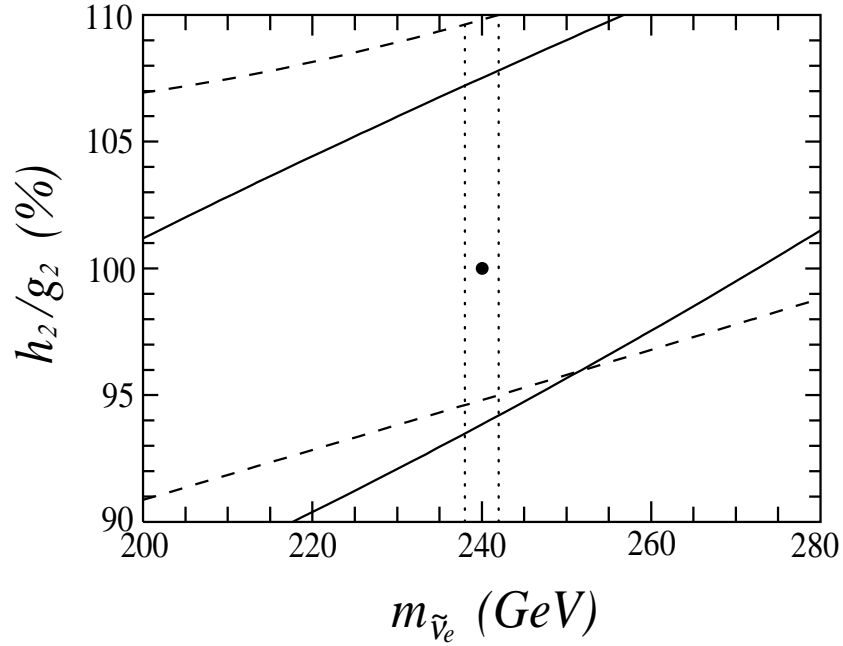


FIG. 4. The same as in Fig. 3, but with underlying parameter  $m_{\tilde{\nu}_e} = 240 \text{ GeV}$ , and dotted contours at  $\Delta m_{\tilde{\nu}_e} = 2 \text{ GeV}$ .

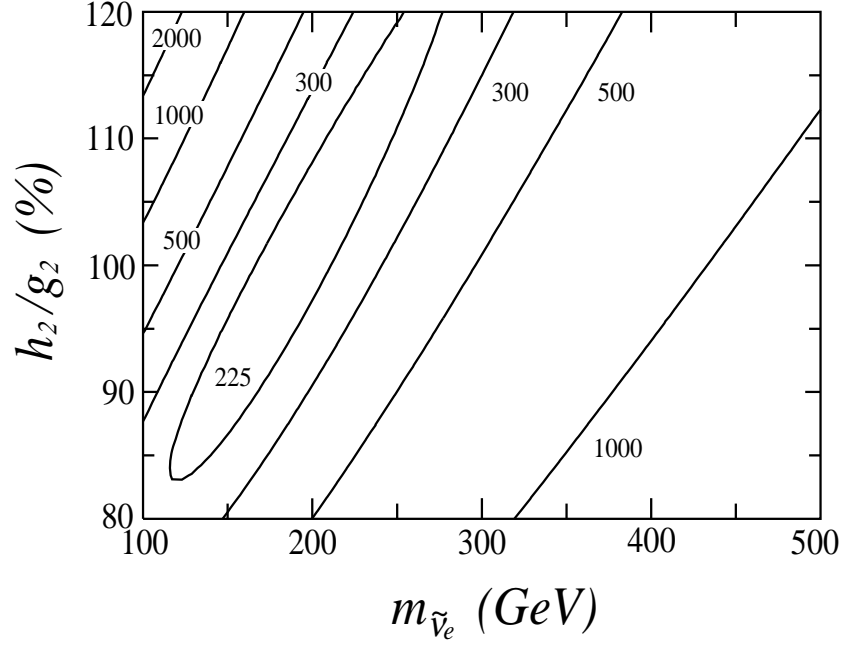


FIG. 5. Same as in Fig. 1, but for  $\sqrt{s} = 400$  GeV.

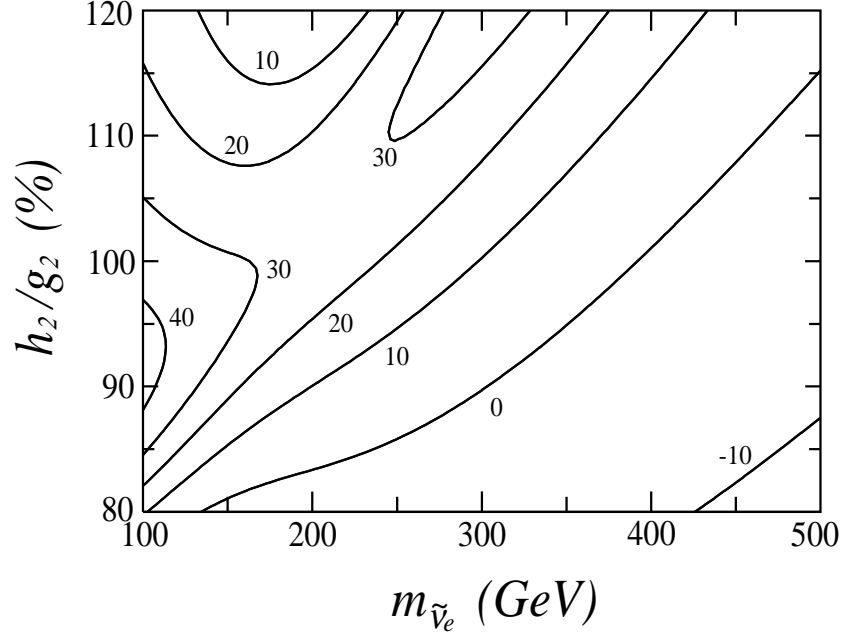


FIG. 6. Same as in Fig. 2, but for  $\sqrt{s} = 400$  GeV.

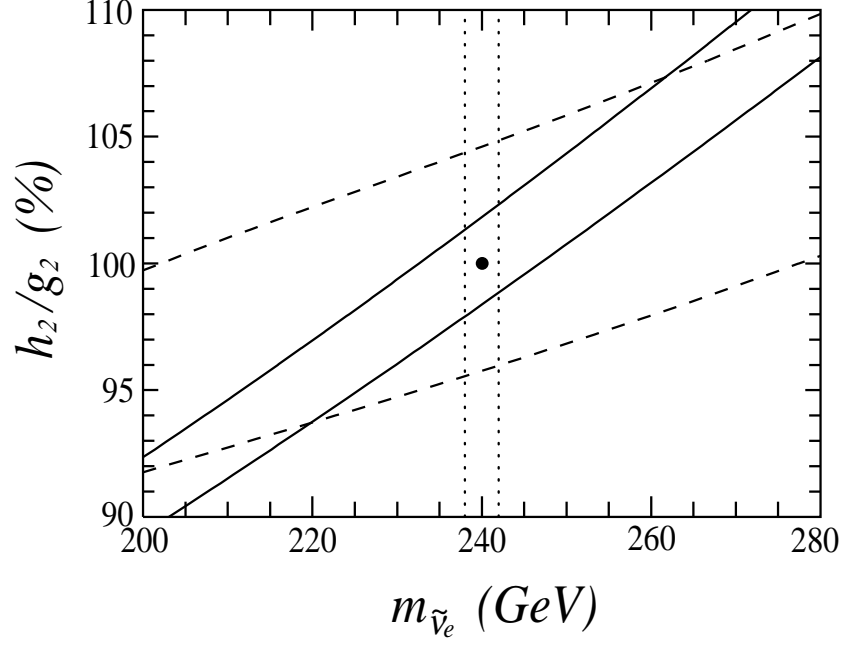


FIG. 7. The same as in Fig. 3, but with underlying parameter  $m_{\tilde{\nu}_e} = 240$  GeV, dotted contours at  $\Delta m_{\tilde{\nu}_e} = 2$  GeV, and improved center-of-mass energy  $\sqrt{s} = 400$  GeV.

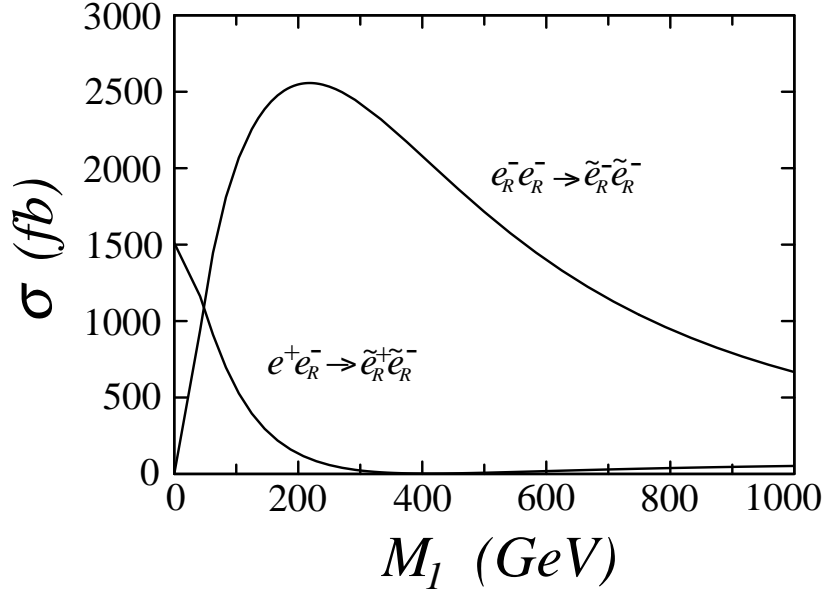


FIG. 8. The total selectron pair production cross sections for the  $e_R^- e_R^-$  and  $e^+ e_R^-$  modes with  $m_{\tilde{e}_R} = 150$  GeV and  $\sqrt{s} = 500$  GeV, as functions of the Bino mass  $M_1$ , assuming the Bino is a mass eigenstate. Note that the very small (but nonzero) cross section for the  $e^+ e_R^-$  mode near  $M_1 \sim 400$  GeV results from destructive interference between the  $s$ - and  $t$ -channel diagrams.



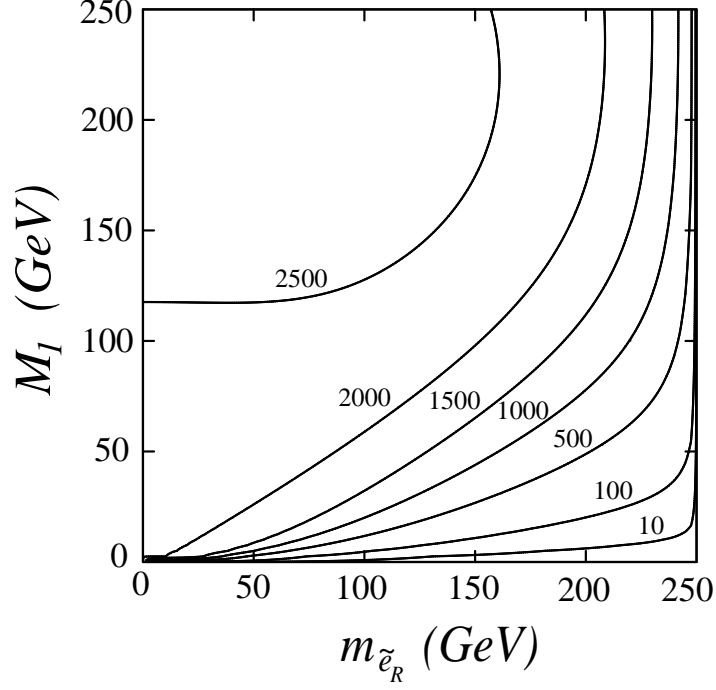


FIG. 9. Contours of constant  $\sigma_R = \sigma(e_R^- e_R^- \rightarrow \tilde{e}_R^- \tilde{e}_R^-)$  in fb in the  $(m_{\tilde{e}_R}, M_1)$  plane for  $\sqrt{s} = 500$  GeV.

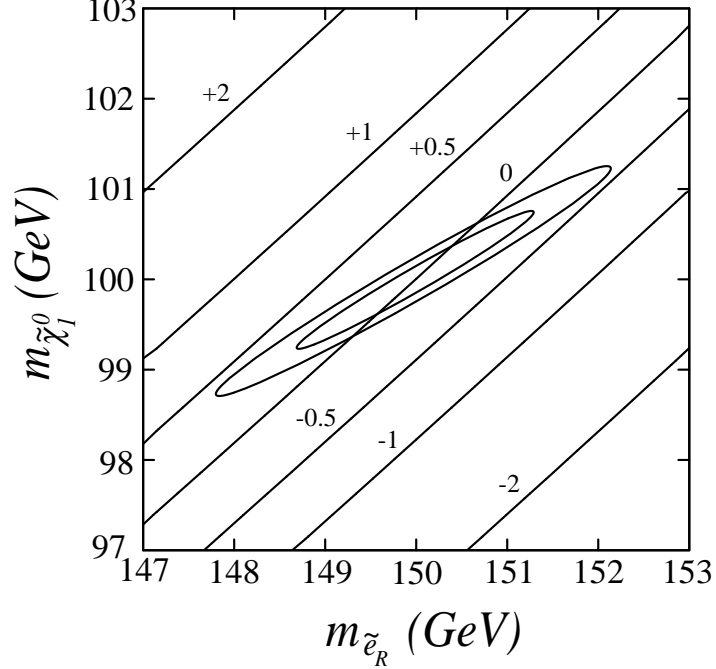


FIG. 10. The allowed regions, “uncertainty ellipses,” of the  $(m_{\tilde{e}_R}, m_{\tilde{\chi}_1^0})$  plane, determined by measurements of the end points of final state electron energy distributions with uncertainties  $\Delta E = 0.3$  GeV and  $0.5$  GeV. The underlying central values are  $(m_{\tilde{e}_R}, m_{\tilde{\chi}_1^0}) = (150 \text{ GeV}, 100 \text{ GeV})$ , and  $\sqrt{s} = 500$  GeV. We also superimpose contours (in percent) of the fractional variation of  $\sigma_R$  with respect to its value at the underlying parameters.

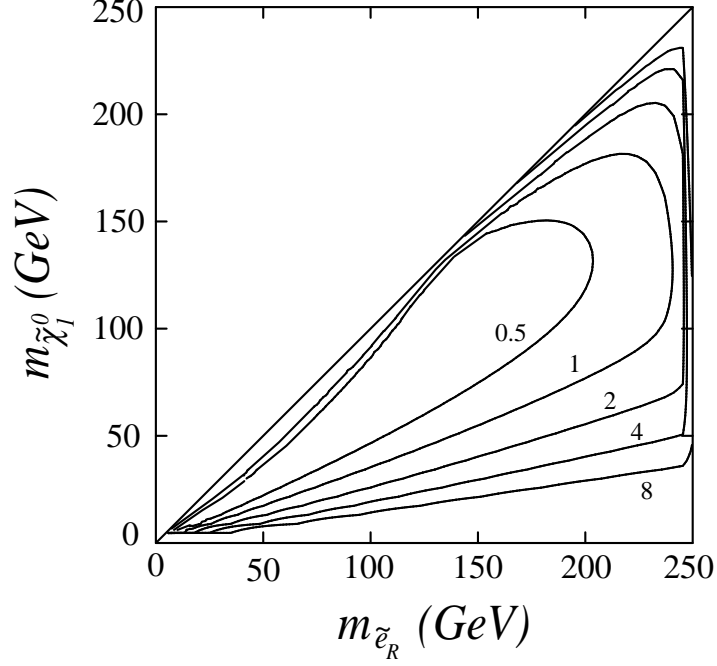


FIG. 11. Contours in the  $(m_{\tilde{e}_R}, m_{\tilde{\chi}_1^0})$  plane of maximal fractional variation in  $\sigma_R$  (in percent) on the  $\Delta E = 0.3$  GeV “uncertainty ellipse,” with  $\sqrt{s} = 500$  GeV.

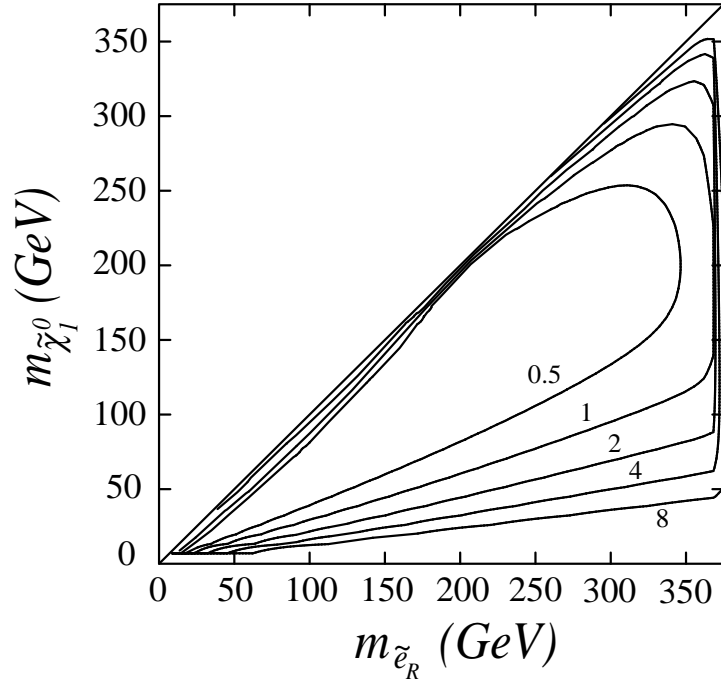


FIG. 12. The same as in Fig. 11, but with  $\sqrt{s} = 750$  GeV. Note the different scales of the axes relative to Fig. 11.

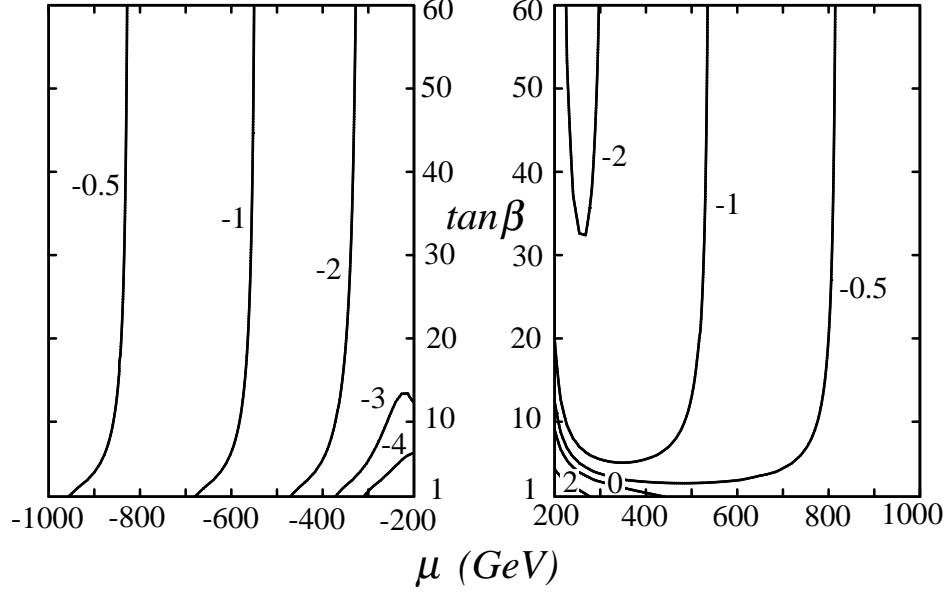


FIG. 13. The fractional variation in  $\sigma_R$  (in percent) in the  $(\mu, \tan \beta)$  plane, with respect to the  $\mu \rightarrow \infty$  limit, for  $(m_{\tilde{e}_R}, m_{\tilde{\chi}_1^0}) = (150 \text{ GeV}, 100 \text{ GeV})$ , with  $\sqrt{s} = 500 \text{ GeV}$ .  $M_2$  is assumed to be  $2M_1$ , and for each point in the plane, their values are fixed by  $m_{\tilde{\chi}_1^0}$ .

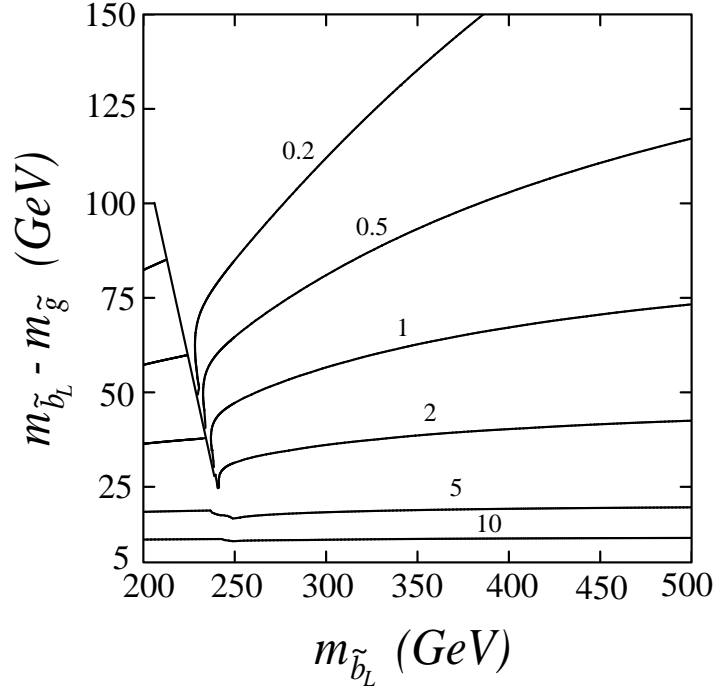


FIG. 14. Systematic uncertainty in  $\tilde{U}_{32}$  arising from uncertainty in  $m_{\tilde{b}_L}$ . Plotted are contours of constant variation in  $\tilde{U}_{32}$  per GeV variation in  $m_{\tilde{b}_L}$ ,  $\frac{\Delta \tilde{U}_{32}}{\Delta m_{\tilde{b}_L}}$ , in percent for  $\sqrt{s} = 1 \text{ TeV}$  in the  $(m_{\tilde{b}_L}, m_{\tilde{b}_L} - m_{\tilde{g}})$  plane. Some regions of this plane correspond to gluino masses that are already excluded by current bounds.

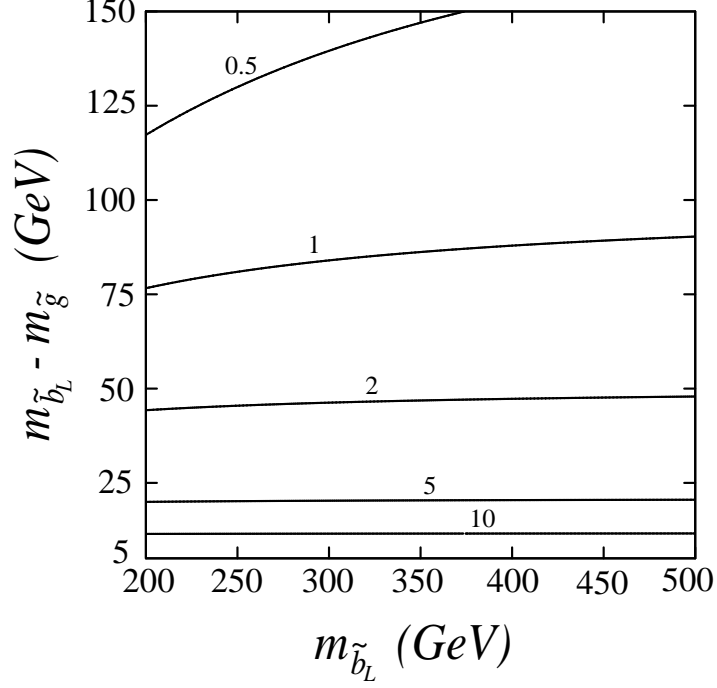


FIG. 15. Systematic uncertainty in  $\tilde{U}_{32}$  arising from uncertainty in  $m_{\tilde{g}}$ . Plotted are contours of constant variation in  $\tilde{U}_{32}$  per GeV variation in  $m_{\tilde{g}}$ ,  $\frac{\Delta\tilde{U}_{32}}{\Delta m_{\tilde{g}}}$ , in percent in the  $(m_{\tilde{b}_L}, m_{\tilde{b}_L} - m_{\tilde{g}})$  plane for  $\sqrt{s} = 1$  TeV.

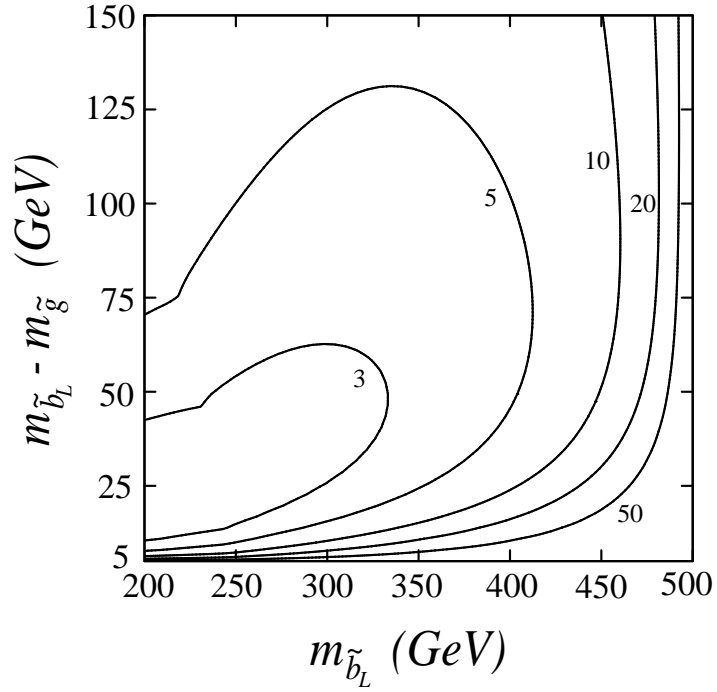


FIG. 16. The error in  $\tilde{U}_{32}$  in percent from statistical uncertainties in the multiple  $b$ -tag events in the  $(m_{\tilde{b}_L}, m_{\tilde{b}_L} - m_{\tilde{g}})$  plane, for  $\sqrt{s} = 1$  TeV and integrated luminosity  $L = 200 \text{ fb}^{-1}$ . The assumed  $b$ -tagging efficiency is  $\epsilon_b = 60\%$ .

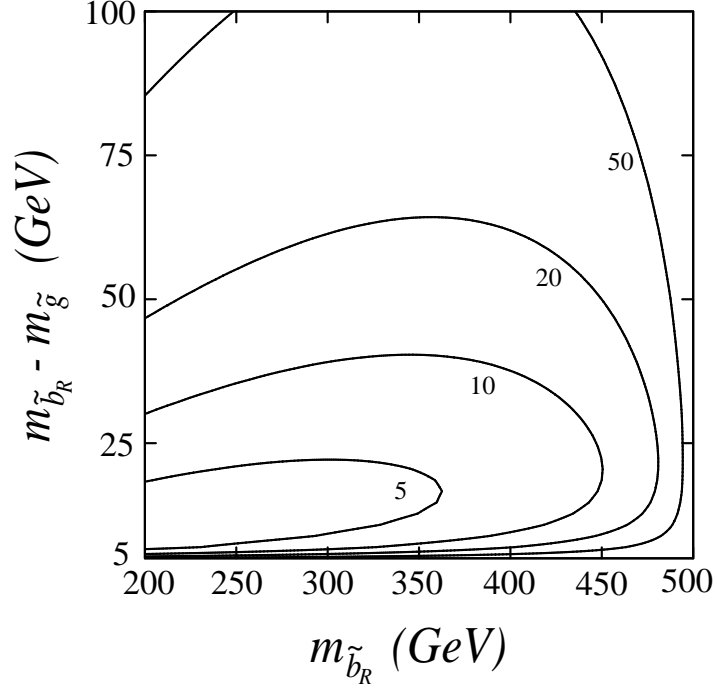


FIG. 17. The error in  $\tilde{U}_{31}$  in percent from the statistical uncertainty in double direct Bino decay events in the  $(m_{\tilde{b}_R}, m_{\tilde{b}_R} - m_{\tilde{g}})$  plane, for  $\sqrt{s} = 1$  TeV. The assumed integrated luminosity is  $L = 200 \text{ fb}^{-1}$ , and the efficiency for the signal is taken to be  $\epsilon = 70\%$ ; the contours scale as  $1/\sqrt{L\epsilon}$ .